Kabashima K, Shiraishi N, Sugita K, Mori T, Onoue A, Kobayashi M, Sakabe J, Yoshiki R, Tamamura H, Fujii N, Inaba K, Tokura Y.	CXCL12-CXCR4 engagement is required for migration of cutaneous dendritic cells.	Am J Pathol	171	1249-57	2007	
Kabashima K, Sugita K, Shiraishi N, Tamamura H, Fujii N, Tokura Y.	CXCR4 engagement promotes dendritic cell survival and maturation.	Biochem Biophys Res Commun	361	1012-6	2007	*
Nagamachi M, Sakata D, Kabashima K, Furuyashiki T, Murata T, Segi-Nishida E, Soontrapa K, Matsuoka T, Miyachi Y, Narumiya S.	Facilitation of Th1-mediated immune response by prostaglandin E receptor EP1.	J Exp Med	204	2865-74	2007	*
Nishio D, Izu K, Kabashima K, Tokura Y.	T cell populations propagating in the peripheral blood of patients with drug eruptions.	J Dermatol Sci	48	25-33	2007	
Sugita K, Kabashima K, Atarashi K, Shimauchi T, Kobayashi M, Tokura Y.	Innate immunity mediated by epidermal keratinocytes promotes acquired immunity involving Langerhans cells and T cells in the skin.	Clin Exp Immunol	147	176-83	2007	

書籍

著者氏名	論文タイトル名	書籍全体の編集者名	書　籍　名	出版社名	出版地	出版年	ページ
Anthony L. DeFranco, Richard M. Locksley, Miranda Robertson(翻訳:小笠原康悦, 監訳:笹月健彦)	Chapter 8, Specialized Lymphocytes in Early Responses and Homeostasis	Anthony L. DeFranco, Richard M. Locksley, Miranda Robertson	Immunity –The Immune Response in Infectious and Inflammatory Disease	Oxford University Press	London	in press	
小笠原康悦	自然免疫と適応免疫を繋ぐNK細胞群	谷口 維紹　山本和彦	The Frontiers in Medical Sciences「免疫応答と免疫病態の統合的分子理解に向けて」	南山堂	東京	2007	42-52
Tadashi Nishiya and Anthony L. DeFranco	Use of Toll-Like Receptor Chimeras to Dissect Mechanisms of Receptor Localization and Signaling.	Gregory W. Konat	SIGNALING BY TOLL-LIKE RECEPTORS	CRC Press	Boca Raton	2008	109-130
戸倉新樹	皮膚T細胞性リンパ腫とケモカイン受容体.	宮地良樹	WHAT'S NEW in 皮膚科学	メディカルレビュー社	東京	2008	114-115
戸倉新樹	光アレルギーとは？	宮地良樹	スキンケア最前線.	メディカルレビュー社	東京	2008	158-159
戸倉新樹	薬剤性光線過敏症.	森田明理他	1冊でわかる光皮膚科学	文光堂	東京	2008	130-134
戸倉新樹	光線過敏型薬疹	池澤善郎, 相原道子	薬疹のすべて	南江堂	東京	2008	222-227

戸倉新樹	光線過敏症と起こしうる皮膚科治療薬は？	宮地良樹, 大谷道輝	現場の疑問に答える皮膚病治療薬	中外医学社	東京	2008	293-294
戸倉新樹	物理化学的皮膚障害・光線過敏症.		皮膚科典型アトラス560	日本医事新報社	東京	2008	61-66
戸倉新樹	アレルギー・マーチって何？皮膚科医の立場から.	宮地良樹他	小児の皮膚トラブル FAQ.編	診断と治療社	東京	2008	100-101
Tokura Y, Moriwaki S	Photodynamic therapy.	Edit. Krieg T et al	Therapy of Skin Diseases	Springer	Berlin	2009	105-111
戸倉新樹	悪性萎縮性丘疹症. 栄養性潰瘍. 壊疽性膿皮症. 柑皮症. 好酸球性血管リンパ球増殖症. 術後紅皮症. 播種状環状肉芽腫. ホジキン肉腫	渡邉 圭二編	医学書院医学大辞典	医学書院	東京	2009	pp11,pp236,pp256,pp548,pp891,pp1281, pp2236, pp2607
戸倉新樹	多形滲出性紅斑・Stevens-Johnson 症候群・蚊アレルギー（蚊刺過敏症）	宮地良樹、古川福実編	皮膚疾患診療実践ガイド第2版	文光堂	東京	2009	pp319-322、pp607-608
戸倉新樹	物理化学的皮膚障害・光線過敏症		知っておきたい画像所見皮膚疾患	日本医事新報社	東京	2009	（印刷中）
戸倉新樹	乾燥肌（ドライスキン）	宮地良樹ら編	美容皮膚科学改訂2版	南山堂	東京	2009	pp560-568
戸倉新樹	顔面のリンパ腫を見逃さない	宮地良樹編	顔の皮膚病最前線	メディカルレビュー社	東京	2009	pp240-243
戸倉新樹	EB ウイルス感染症の皮膚症状は？	宮地良樹編	うつる皮膚病最前線	メディカルレビュー社	東京	2009	pp68-73
戸倉新樹	菌状息肉症・セザリー症候群・原発性皮膚 CD30 陽性 T 細胞増殖性疾患	押味和夫監修	WHO 分類によるリンパ系腫瘍の病態学	中外医学社	東京	2009	pp347-362
戸倉新樹	抗ヒスタミン薬抵抗性の痒みの対策も含めたアトピー性皮膚炎の痒みの治療ポイントは？	秋山一男／他編	EBM アレルギー疾患の治療 2010-2011	中外医学社	東京	2009	pp300-302
椛島健治	プリックテスト、スクラッチテスト、皮内テスト	宮地良樹、古川福美	皮膚科疾患診療実践ガイド（第二版）	文光堂	東京	2009	122-124

椛島健治	皮内テストI-特殊反応	宮地良樹、古川福美	皮膚科疾患診療実践ガイド（第二版）	文光堂	東京	2009	124-125
椛島健治	パッチテスト	宮地良樹、古川福美	皮膚科疾患診療実践ガイド（第二版）	文光堂	東京	2009	130-131
椛島健治	リンパ球検査、リンパ球幼若化試験	宮地良樹、古川福美	皮膚科疾患診療実践ガイド（第二版）	文光堂	東京	2009	134-136
椛島健治	外的刺激が起こす皮膚の免疫反応	戸倉新樹	皮膚科診療プラクティス20 Environmental Dermatology	文光堂	東京	2007	8-13
椛島健治	抗炎症作用のある抗菌剤	宮地良樹	what's new in 皮膚科学 2008-2009	メジカルビュー社	東京	2008	70-71
椛島健治	光線過敏症	山口徹、福井次矢、北原光夫	今日の治療指針 2009	医学書院	東京	2008	878-880
椛島健治	紫外線と表皮角化細胞	森田明理	一冊でわかる光皮膚科	文光堂	東京	2008	14-16

IV. 研究成果の刊行物・別刷

Tim-3 mediates phagocytosis of apoptotic cells and cross-presentation

Masafumi Nakayama,[1] Hisaya Akiba,[1] Kazuyoshi Takeda,[1] Yuko Kojima,[2] Masaaki Hashiguchi,[3] Miyuki Azuma,[3] Hideo Yagita,[1] and Ko Okumura[1]

[1]Department of Immunology and [2]Division of Biomedical Imaging Research, Biomedical Research Center, Juntendo University School of Medicine, Tokyo; and [3]Department of Molecular Immunology, Graduate School, Tokyo Medical and Dental University, Tokyo, Japan

Phagocytes such as macrophages and dendritic cells (DCs) engulf apoptotic cells to maintain peripheral immune tolerance. However, the mechanism for the recognition of dying cells by phagocytes is not fully understood. Here, we demonstrate that T-cell immunoglobulin mucin-3 (Tim-3) recognizes apoptotic cells through the FG loop in the IgV domain, and is crucial for clearance of apoptotic cells by phagocytes. Whereas Tim-4 is highly expressed on peritoneal resident macrophages, Tim-3 is expressed on peritoneal exudate macrophages, monocytes, and splenic DCs, indicating distinct Tim-mediated phagocytic pathways used by different phagocytes. Furthermore, phagocytosis of apoptotic cells by CD8 DCs is inhibited by anti–Tim-3 mAb, resulting in a reduced cross-presentation of dying cell-associated antigens in vitro and in vivo. Administration of anti–Tim-3 as well as anti–Tim-4 mAb induces autoantibody production. These results indicate a crucial role for Tim-3 in phagocytosis of apoptotic cells and cross-presentation, which may be linked to peripheral tolerance. (Blood. 2009;113: 3821-3830)

Introduction

Apoptosis is a crucial process in the development and homeostasis of multicellular organisms.[1,2] In the immune system, an enormous number of cells undergo apoptosis during development of lymphocytes and after interaction with antigens.[3] Because apoptotic cells and secondary necrotic cells releasing intracellular contents could be autoantigens, phagocytes such as macrophages and dendritic cells (DCs) must engulf these dying cells rapidly and efficiently to prevent detrimental inflammatory responses and autoimmunity.[1,4] To engulf apoptotic cells, macrophages use a variety of molecules, including Mer tyrosine kinase (MerTK),[5] milk fat globule-EGF-factor 8 (MFG-E8),[6] brain-specific angiogenesis inhibitor 1 (BAI1),[7] and T-cell immunoglobulin and mucin domain-containing molecule 4 (Tim-4).[8,9] However, their relative contributions to the phagocytosis remain to be elucidated. Multiple receptors may simultaneously recognize multiple "eat-me" signals on apoptotic cells. In addition, different subsets of macrophages may use different repertoires of receptors for the phagocytosis.

DCs are able to not only phagocytose apoptotic cells but also present dying cell-associated antigens with MHC class I molecules, which is termed as "cross-presentation."[1,10] It has been considered that, in steady state, cross-presentation of self-antigens by DCs stimulates CD8 T cells to proliferate abortively, resulting in their deletion, which is crucial to maintain peripheral tolerance.[10-14] Among mouse splenic DC subsets, CD8 DCs are unique in their ability for efficient phagocytosis of apoptotic cells and cross-presentation.[15,16] However, the mechanism for the recognition of apoptotic cells by CD8 DCs is poorly understood. Scavenger receptor CD36 and mannose receptor (MR)/DEC205 are highly expressed on CD8 DCs, but not CD8 DCs, however, these receptors are not required for cross-presentation of cell-associated antigens by this DC subset.[16-18] Neither $_{v}$ $_{3}$ nor $_{v}$ $_{5}$ integrin that mediates phagocytosis of apoptotic cells by macrophages[1] is essential for phagocytosis by CD8 DCs.[17] Thus, the phagocytic receptor for apoptotic cells linked to cross-presentation remains to be identified.

Tim-3 has been identified as a Th1-specific marker, and several in vivo studies have shown that Tim-3 regulates autoimmunity.[19,20] We and others have reported that Tim-3 negatively regulates Th1-mediated inflammatory diseases such as experimental autoimmune encephalomyelitis (EAE), type I diabetes, and acute graft-versus-host diseases (aGVHD).[21-23] Moreover, it has been reported that Tim-3 promotes tolerance induction.[21,22] Recently, Zhu et al have identified galectin-9 as a Tim-3 ligand, and they have demonstrated that galectin-9 binds to the carbohydrate chains on Tim-3, and induces cell death of Th1 cells in vitro, which may explain the mechanism by which Tim-3 suppresses Th1 immunity.[24] On the other hand, Anderson et al have reported that Tim-3 is expressed on DCs, and that galectin-9 activates the DCs through Tim-3, proposing that Tim-3 exacerbates EAE.[25] Taken together, Tim-3 appears to have multiple roles for the immune regulation in vivo, however, it remains unknown whether these multiple functions of Tim-3 are mediated solely through galectin-9.

In this study, we demonstrate that Tim-3 recognizes apoptotic cells through the FG loop in the IgV domain. Although Tim-4 is reported to be crucial for the phagocytosis of apoptotic cells by peritoneal macrophages,[8,9] we highlight here Tim-3 as the phagocytic receptor responsible for cross-presentation of dying cell-associated antigens by CD8 DCs. We propose that this novel function of Tim-3 may be involved in autoimmune regulation and tolerance induction.

Submitted October 23, 2008; accepted February 5, 2009. Prepublished online as *Blood* First Edition paper, February 17, 2009; DOI 10.1182/blood-2008-10-185884.

The online version of this article contains a data supplement.

The publication costs of this article were defrayed in part by page charge payment. Therefore, and solely to indicate this fact, this article is hereby marked "advertisement" in accordance with 18 USC section 1734.

Methods

Mice and reagents

Five-week-old female C57BL/6 mice were obtained from Charles River Japan (Yokohama, Japan). OT-I mice expressing $OVA_{257-264}$/H-2K^b–specific TCR were kindly provided by W. R. Heath (The Walter and Eliza Hall Institute, Melbourne, Australia) through H. Udono (RCAI, RIKEN, Yokohama, Japan). These mice were maintained under specific pathogen-free conditions, and used according to the guidelines of the institutional animal care and use committee established at Juntendo University and Tokyo Medical and Dental University. pcDNA3.1( ), pEF6/V5-TOPO, and pcDNA3.1-GFP-TOPO vectors were purchased from Invitrogen (Frederick, MD). PE-Mac1 (CD11b) mAb and control rat IgG2a were purchased from eBioscience (San Diego, CA). FITC-anti-CD11c mAb, PE-anti-V 2 mAb, and allophycocyanin (APC)–anti-CD8 mAb were purchased from BD Biosciences (San Jose, CA). Alexa Fluor 647–anti-CD8 mAb was purchased from Biolegend (San Diego, CA). 5-(and-6)-Carboxyfluorescein diacetate succinimidyl ester (CFSE) and 5-(and-6)-carboxytetramethylrhodamine succinimidyl ester (TAMRA) were purchased from Invitrogen. TdT and biotin-16-dUTP were purchased from Roche (Indianapolis, IN).

Generation of Tim-Igs and mAbs

The expression vectors for Tim-1–Ig, Tim-2–Ig, Tim-3–Ig, and Tim-4–Ig were generated by linking the extracellular domains of Tim-1 (aa 1-236), Tim-2 (aa 1-230), Tim-3 (aa 1-191), or Tim-4 (aa 1-288) to the Fc portion of mouse IgG2a in the pcDNA3.1( ) vector. Tim-Ig proteins were produced by transfection of each vector into HEK293T cells. The anti–mouse Tim-1 mAb (RMT1-17, rat IgG2a,), Tim-2 mAb (RMT2-14, rat IgG2a,), and Tim-3 mAb (RMT3-23, rat IgG2a,) were generated immunizing SD rats with Tim-1–Ig, Tim-2–Ig, and Tim-3–Ig, respectively, as described before.[23] Likewise, the anti–Tim-4 mAb (RMT4-54, rat IgG2a,) was generated by immunizing an SD rat with Tim-4–Ig, fusing lymph node cells with P3U1 myeloma cells, and screening the binding to CHO cells expressing Tim-4, but not parental CHO cells. For confocal microscopy, RMT3-23 was labeled with Alexa Fluor 594 using the mAb labeling kit (Invitrogen). Requests for mAbs should be addressed to H. Akiba (e-mail: hisaya@juntendo.ac.jp).

Cell lines

A normal rat kidney cell line (NRK-52E) was maintained in complete RPMI medium (RPMI 1640 supplemented with 10% FBS, 100 U/mL penicillin, 100 g/mL streptomycin, and 2 mM glutamine, 10 mM HEPES, and 50 M 2-mercaptoethanol). HEK293T cells (ATCC, Manassas, VA) were maintained in complete DMEM medium (DMEM supplemented with 10% FBS, 100 U/mL penicillin, 100 g/mL streptomycin, and 2 mM glutamine). For construction of expression vectors, the entire coding region of mouse Tim-1, Tim-2, Tim-3, or Tim-4 was subcloned into pMKITneo. Tim-3 cDNA was also subcloned into pEF6/V5-TOPO vector. Several mutant forms were prepared by polymerase chain reaction (PCR)–based mutagenesis using Tim-3/pEF6V5-TOPO as a template. After confirmation of nucleotide sequences, Tim expression vectors were transduced into NRK cells by electroporation with a Gene Pulser (Bio-Rad Laboratories, Hercules, CA). After selection with 1 mg/mL G418, cell surface expression was estimated by respective anti-Tim mAbs. HEK293T cells were transiently transfected with these expression vectors using lipofectAMINE2000 (Invitrogen). Two days after the transfection, cell surface expression of Tim was estimated by flow cytometry.

Phagocytosis assay

For preparation of apoptotic cells, thymocytes from C57BL/6 mice were labeled with 1 M CFSE or 10 g/mL TAMRA, and then were UV irradiated (100 J/cm^2). After UV irradiation, the cells were cultured in complete RPMI for 2 hours at 37°C, and then used for the phagocytosis assay. NRK cells (10^5 per well), NIH3T3 cells (5 10^4 cells per well), and HEK293T cells (10^5 cells per well) were plated onto 24-well plates, which were precoated with poly-L-lysine for HEK293T cells, a day before the phagocytosis assay. These cell lines were incubated with fluorescently labeled apoptotic cells (2 10^6 per well) at 37°C for the indicated periods. The recognition (binding and/or incorporation) of fluorescently labeled apoptotic cells by these cell lines was analyzed by flow cytometry using a FACSCalibur (BD Biosciences) and/or fluorescence microscopy using an Olympus FV1000 laser scanning confocal microscope (Melville, NY) equipped with 40 or 100 objective lens. For macrophages, peritoneal cells were harvested from C57BL/6 mice 3 days after intraperitoneal injection of 2 mL 3% wt/vol thioglycolate, or from untreated mice. These peritoneal cells (5 10^5 per well) were plated onto 48-well plate for 2 hours at 37°C, and then washed with PBS twice to remove floating cells. In some assay, macrophages were preincubated with the indicated mAb (30 g/mL) for 60 minutes at 4°C, and then washed with PBS to remove unbound mAb. Macrophages were cultured with fluorescently labeled apoptotic cells (2.5 10^6 per well) for 30 minutes at 37°C, and then washed with PBS 3 times to remove unbound apoptotic cells. After trypsinization, cells were harvested and stained with PE-Mac1. CFSE fluorescence intensity in Mac1 cells was analyzed on a FACSCalibur (BD Biosciences). As for an in vivo phagocytosis by PEM, sterile peritonitis was induced in C57BL/6 mice by intraperitoneal injection of 3% thioglycolate medium (2 mL per mouse). Three days later, these mice (n 4-5 per group) were treated intraperitoneally with control rat IgG (rIgG), RMT3-23, or RMT4-54 (200 g/mouse). Three hours later, mice were intraperitoneally injected with CFSE-labeled apoptotic cells (10^8 per mouse), and another 2 hours later, peritoneal cells were harvested. The recognition of apoptotic cells by Mac1 cells was analyzed by flow cytometry. For statistic evaluation, the unpaired Student *t* test, 2-tailed was used. *P* values less than .05 were considered significant. For in vitro phagocytosis assay using splenic DCs, spleens were digested with 400 U/mL collagenase (Wako Biochemicals) in the presence of 5 mM EDTA and separated into low- and high-density fractions on Optiprep gradient (Axis-Shield, Oslo, Norway). Low-density cells were purified using anti-CD11c MACS beads (Miltenyi Biotec, Auburn, CA). After staining CD11c cells with APC-anti-CD8 mAb, these cells (5 10^5 per well) were cocultured with TAMRA-labeled apoptotic cells (2.5 10^6 per well) in 48-well plate for the indicated periods, and then the cells were stained with FITC–anti-CD11c mAb. TAMRA fluorescence intensity in CD8 CD11c and CD8 CD11c cells was analyzed on a FACSCalibur. As for in vivo phagocytosis by splenic DCs, mice (n 3 per group) were treated intravenously with rIgG, or RMT3-23 and/or RMT4-54 (200 g each/mouse), and then 2 hours later, with CFSE-labeled apoptotic splenocytes (2 10^7 per mouse). Mice were killed at the indicated time points, and the recognition of apoptotic cells by CD8 CD11c cells was analyzed by flow cytometry. For statistic evaluation, the unpaired Student *t* test, 2-tailed was used. *P* values less than .05 were considered significant.

In situ identification of nuclear DNA fragmentation

C57BL/mice (n 4-6 per group) were treated intraperitoneally with rIgG, or RMT3-23 and/or RMT4-54 (200 g each per mouse) twice a week for 4 weeks. Three days after the final injection, mice were killed. Serum was stocked for measurement of anti-dsDNA antibody levels. Brain, liver, spleen, and pancreas were immersion-fixed in 20% buffered formalin and embedded in paraffin. After being deparaffinized, tissue sections were stained using in situ TUNEL method with biotin-16-dUTP (Roche Diagnostics, Basel, Switzerland) and diaminobenzidine as a peroxidase substrate. Nuclei were counterstained with hematoxylin. The number of TUNEL-positive cells was quantified with KS400 Image Analysis System (KS400; Zeiss, Heidelberg, Germany).

Measurement of anti-dsDNA antibody levels in serum

Serum levels of anti-dsDNA IgG were determined as described previously.[26] In brief, enzyme-linked immunosorbent assay (ELISA) plates were coated with 5 g/mL dsDNA derived from calf thymus (Sigma-Aldrich, St Louis, MO). Anti-dsDNA antibody level was expressed in units, referring to

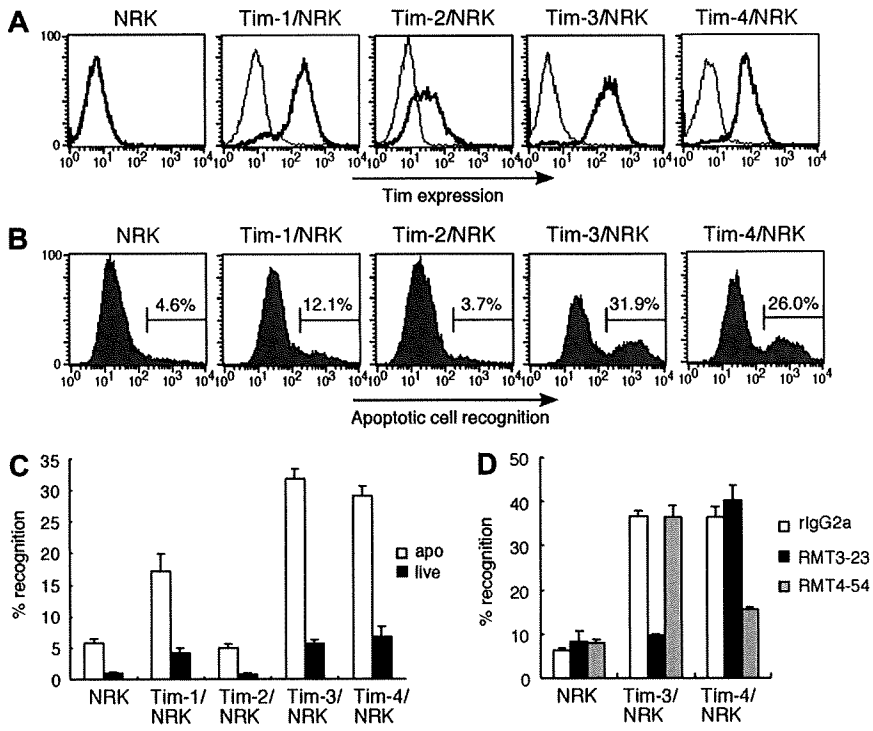

Figure 1. Tim-3 recognizes apoptotic cells. (A) NRK cells stably expressing Tim-1, Tim-2, Tim-3, or Tim-4 were stained with biotinylated anti–Tim-1 mAb (RMT1-17), anti–Tim-2 mAb (RMT2-14), anti–Tim-3 mAb (RMT3-23), or anti–Tim-4 mAb (RMT4-54), respectively. Parental NRK cells were stained with a cocktail of all mAbs. Then cells were stained with PE-avidin, and analyzed by flow cytometry (thick histogram). Thin histograms indicate background staining with control rat IgG2a, followed by PE-avidin. (B) These NRK cells were cultured with CFSE-labeled apoptotic cells for 30 minutes at 37°C. Recognition of apoptotic cells by these NRK cells was quantified by flow cytometry. (C) These NRK cells were cultured with CFSE-labeled viable cells or apoptotic cells for 30 minutes at 37°C. Percentage of the recognition was quantified by flow cytometry. Data are represented as mean SD of triplicates. (D) These NRK cells were pretreated with 20 g/mL control rIgG2a, RMT3-23, or RMT4-54 mAb, and then cultured with CFSE-labeled apoptotic cells for 30 minutes at 37°C. Percentage of the recognition was quantified by flow cytometry. Data are represented as mean SD of triplicates. Similar results were obtained in 3 (A-C) or 2 (D) independent experiments.

standard curve obtained by serial dilution of a standard serum pool from (NZB NZW) F1 mice older than 8 months, containing 1000 U activities/mL (kindly provided by S. Hirose, Juntendo University).

Flow cytometric analysis for Tim expression

Mouse macrophages or low-density splenocytes were pretreated with anti-FcR mAb (2.4G2), and then were incubated with 0.5 g biotinylated mAb for 30 minutes at 4°C, followed by PE-streptavidin and FITC-anti-CD11b mAb (for macrophages) or PE-streptavidin, FITC–anti-CD11c mAb and APC–anti-CD8 mAb (for splenic DCs). After washing with PBS, Tim expression on CD11b , CD8 CD11c , or CD8 CD11c cells was analyzed on a FACSCalibur, and the data were analyzed using the CellQuest program (BD Biosciences).

In vitro cross-presentation assay

OVA-loaded dying cells were prepared by osmotic shock as described previously.[12] For splenic DC subsets, CD11c cells purified using anti-CD11c MACS beads (92% CD11c) were then stained with FITC–anti-CD11c and APC–anti-CD8 mAbs, followed by sorting into subsets (89% CD8 CD11c ; 98% CD8 CD11c) on FACSVantage (BD Biosciences). OVA-loaded (10 mg/mL) dying cells (2.5 10^6 per well) were cocultured with CD8 DCs or CD8 DCs (5 10^5 per well) in presence of rIgG, RMT3-23, or RMT4-54 (30 g/mL) on 48-well plate for 1.5 hours, and then DCs were sorted again using anti-CD11c MACS beads. CD8 or CD8 DCs (both 10^4 or 2 10^3 per well) were cocultured with purified OT-I CD8 T cells (10^5 per well) in 96-well flat-bottom plate. For the direct presentation, CD8 or CD8 DCs (10^4 per well) were cocultured with 1 nM $OVA_{257-264}$ SIINFEKL peptides (AnaSpec, San Jose, CA) and OT-I CD8 T cells (10^5 per well) in presence of rIgG, RMT3-23, or RMT4-54 (30 g/mL) in 96-well flat-bottom plate. Two days later, 50 L supernatant was harvested and tested for IFN- production by sandwich ELISA (eBioscience). The cultures were then pulsed overnight with [^{3}H]thymidine (0.5 Ci [0.0185 MBq]/well; GE Healthcare, Little Chalfont, United Kingdom) and the uptake was measured in a microbeta counter (Microbeta Plus; Wallac, Turku, Finland).

In vivo cross-presentation assay

In vivo cross-presentation assay was performed as described previously[27] with minor modifications. CFSE-labeled OT-I cells (2 10^6 per mouse) were transferred intravenously into B6 mice. Next day, mice were injected intravenously with rIgG, or RMT3-23 and/or RMT4-54 (200 g each per mouse), and then 2 hours later, with OVA-loaded (1 mg/mL) dying splenocytes (10^7 per mouse). Two days later, mice were killed, and splenocytes were stained with PE–anti-V 2 and APC–anti-CD8. CFSE fluorescence intensity of CD8 V 2 cells was analyzed by flow cytometry.

Results

Tim-3 recognizes apoptotic cells and is recruited to phagosome

Because Tim-4 and Tim-1 are recently reported to recognize apoptotic cells,[8,9] we first verified the binding activity of NRK cells stably expressing Tim family molecules (Figure 1A) to apoptotic cells. As for apoptotic cells, we used UV (100 J/cm^2)–irradiated thymocytes because these cells show typical apoptotic phenotypes, which are annexin V and propidium iodide negative (PI) (Figure S1A, available on the *Blood* website; see the Supplemental Materials link at the top of the online article), and do not express Tim molecules (Figure S1B), excluding Tim-Tim interaction in this study. In addition to Tim-4/NRK and Tim-1/NRK, we found that Tim-3/NRK also efficiently bound apoptotic cells, but not live cells (Figure 1B,C), and that the binding of Tim-3/NRK and Tim-4/NRK cells to apoptotic cells was abrogated by anti–Tim-3 mAb RMT3-23 and anti–Tim-4 mAb RMT4-54, respectively (Figure 1D). These results suggest that Tim-3 as well as Tim-4 acts as a receptor for apoptotic cells.

To further address whether expression of Tim-3 could confer the ability to internalize or just bind apoptotic cells, we next used HEK293T cell reconstitution system because although ectopic expression of an authentic phagocytic receptor Fc RIII with FcR chain enabled this cell line to internalize IgG-opsonized bacteria, the expression of scavenger receptor-A (SR-A)[28] or paired Ig-like receptor-B (PIR-B),[29] which is the nonphagocytic receptor for bacteria, conferred the binding without significant internalization (not shown). As shown in

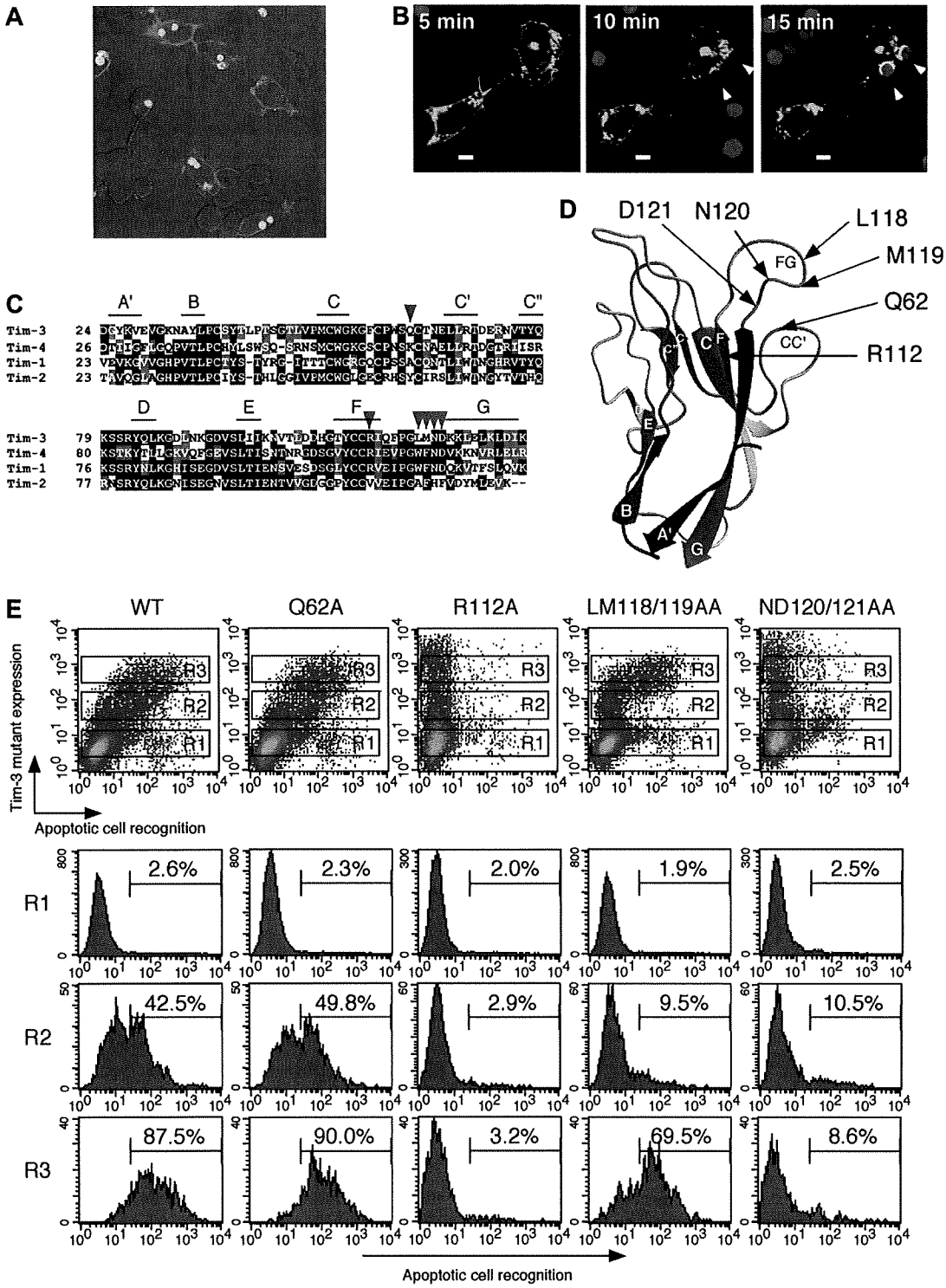

Figure 2. Tim-3 internalizes apoptotic cells through the FG loop in IgV domain. (A) HEK293T cells transiently expressing Tim-3 were cultured with CFSE-labeled apoptotic cells for 60 minutes at 37°C, and then cells were stained with biotinylated RMT3-23 and Alexa 594–avidin. (B) TAMRA-labeled apoptotic cells were added to HEK293T cells transiently expressing Tim-3-GFP under fluorescence microscope. Phagocytosis and Tim-3-GFP localization were analyzed at the indicated time points. White arrowheads indicate apoptotic cells internalized via Tim-3. White bars indicate 5 m. (C) Alignment of IgV domain of Tim family molecules. The -strands of Tim-3 were shown with lines. Mutated residues were indicated by red arrowheads. (D) Positions of mutated residues are indicated on 3-dimensional structure of Tim-3 IgV domain. The color of the protein main-chain is gradually changed along the sequence from blue (N-terminal) to red (C-terminal). (E) HEK293T cells transiently expressing wild-type or mutant Tim-3 were cultured with CFSE-labeled apoptotic cells for 60 minutes at 37°C, and then cells were stained with biotinylated RMT3-23 and PE-avidin. Recognition of apoptotic cells by gated HEK293T cells (R1; Tim-3 , R2; Tim-3^{low}, R3; Tim-3^{high}) was analyzed by flow cytometry. Similar results were obtained in 2 (A,B) or 3 (E) independent experiments.

Figure 2A, Tim-3–positive cells efficiently internalized CFSE-labeled apoptotic cells, indicating that Tim-3 is a phagocytic receptor for apoptotic cells. Furthermore, we addressed Tim-3 localization upon initial contact with apoptotic cells. To visualize Tim-3, we generated an expression vector for Tim-3 fused at its C-terminus to green fluorescence protein (GFP), and then expressed this fusion receptor in HEK293T cells. Whereas Tim-3 was mostly expressed at the cell surface in resting

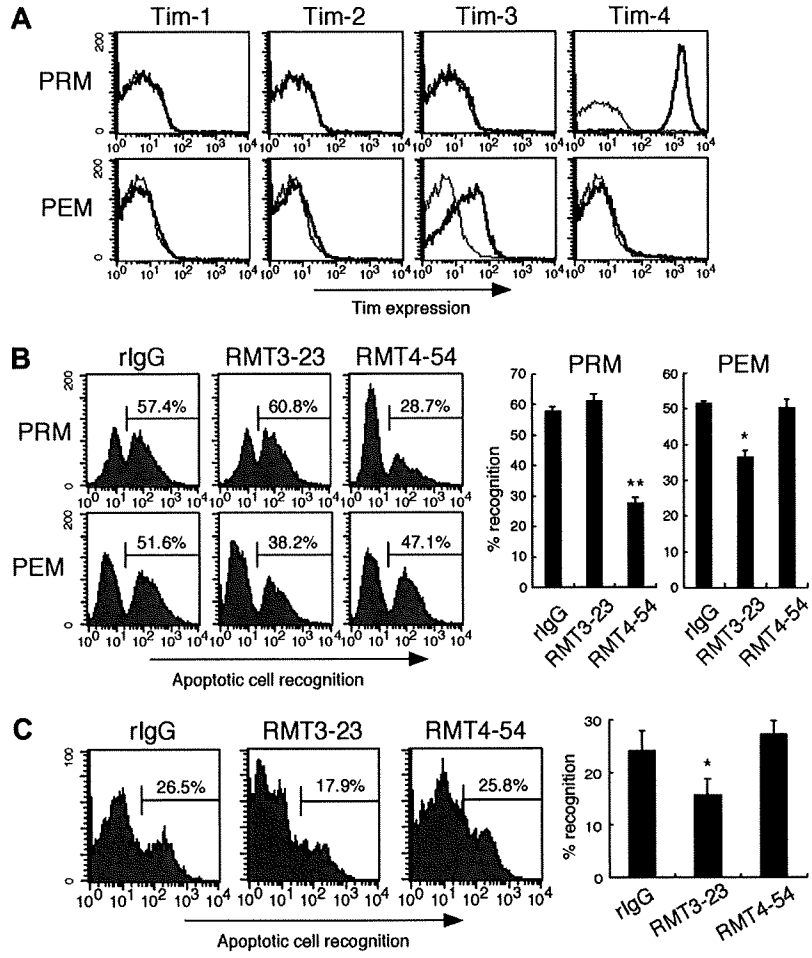

Figure 3. Tim-3 mediates phagocytosis of apoptotic cells by peritoneal exudate macrophages. (A) Peritoneal resident Mac1 cells (PRMs) and peritoneal exudate Mac1 cells (PEMs) were stained with biotinylated RMT1-17, RMT2-14, RMT3-23, or RMT4-54, followed by FITC-anti-CD11b mAb and PE-avidin (thick histograms); then CD11b cells were analyzed by flow cytometry. Thin histograms indicate background staining with biotinylated control rat IgG2a. (B) Macrophages were pretreated with control rat IgG2a (rIgG), RMT3-23, or RMT4-54, and then cultured with CFSE-labeled apoptotic cells for 30 minutes at 37°C. Cells were stained with PE-Mac1, and percentage of recognition of CFSE-apoptotic cells by Mac1 cells was quantified by flow cytometry. Columns represent mean SD of triplicates (*P .05; **P .01 compared with rIgG). (C) Peritonitis was elicited by intraperitoneal injection of thioglycolate. Three days later, the mice were intraperitoneally injected with rIgG, RMT3-23, or RMT4-54 (200 g/head), and then with CFSE-labeled apoptotic cells. Two hours later, peritoneal cells were harvested, and recognition of CFSE-labeled apoptotic cells by Mac1 cells was quantified by flow cytometry. The experiments (n 4-5 per group) were performed 3 times independently with a similar result. Columns represent mean SD of 4 mice in a representative experiment (*P .05 compared with rIgG). Similar results were obtained in 3 (A,C) or 2 (B) independent experiments.

conditions, upon recognition of TAMRA-labeled apoptotic cells, Tim-3 was recruited to the phagocytic cup (Figure 2B). This substantiates that Tim-3 mediates engulfment of apoptotic cells.

Tim-3 binds to PS

We next addressed whether Tim-3 also binds to phosphatidylserine (PS), a major "eat-me" signal,[1,2] by solid-phase ELISA using soluble Ig fusion proteins with extracellular domains including both IgV and mucin domains of Tim-2, Tim-3, and Tim-4. In addition to the strong binding of Tim-4-Ig to PS, we observed that Tim-3–Ig weakly but substantially bound to PS, but not other phospholipids such as phosphatidylethanolamine (PE), phosphatidylinositol (PI), and phosphatidylcholine (PC) (Figure S2A). Tim-2–Ig did not bind any phospholipids even at a high dose. The Tim-3–Ig or Tim-4–Ig binding to PS was abrogated by RMT3-23 or RMT4-54, respectively, in a dose-dependent manner (Figure S2B). These results indicate that Tim-3 recognizes PS, although the affinity is lower than that of Tim-4.

Tim-3 recognizes apoptotic cells through the FG loop in IgV domain

We next explored the Tim-3 recognition site of apoptotic cells. Recently, Santiago et al have revealed a crystal structure of Tim-4 and demonstrated that Tim-4 binds PS through the metal ion–dependent ligand binding site (MILIBS) in the FG loop, which is conserved in all Tim family members except Tim-2.[30] Thus, we specifically mutated some of amino acids locating around the FG loop of Tim-3 to alanine, and transiently transfected HEK293T cells with each mutant construct to address the relationship between expression level of each mutant and their phagocytic activities. We first replaced Gln62 or Arg112 to Ala because these amino acids, which locate in FG-CC cleft in the 3D structural model of Tim-3 IgV domain (Figure 2C,D), are critical for galectin-9–independent ligand binding.[31] Substitution of Gln62 did not alter the phagocytic activity, although substitution of Arg112 completely abrogated the activity (Figure 2E). We next addressed the putative MILIBS, which locates on the FG surface loop (Figure 2D). The LM118/119AA mutant recognized apoptotic cells only at high expression level, suggesting that substitution of these residues to both Ala weakened the activity (Figure 2E). The ND120/121AA mutant completely lost the activity (Figure 2E). These results suggest that Tim-3 internalizes apoptotic cells through the FG loop in IgV domain, and that at least in part galectin-9–independent ligand binding[31] might be linked to recognition of apoptotic cells.

Tim-3 and Tim-4 mediate phagocytosis of apoptotic cells by distinct macrophage subsets

We next examined the cell surface expression of Tim molecules on mouse primary macrophages, and their contribution to the phagocytosis of apoptotic cells. We found Tim-3 expression on peritoneal exudate Mac1 cells (PEMs), but not peritoneal resident Mac1 cells (PRMs) from naive mice (Figure 3A). In contrast, Tim-4 was highly expressed on PRMs, but not PEMs, which is consistent with

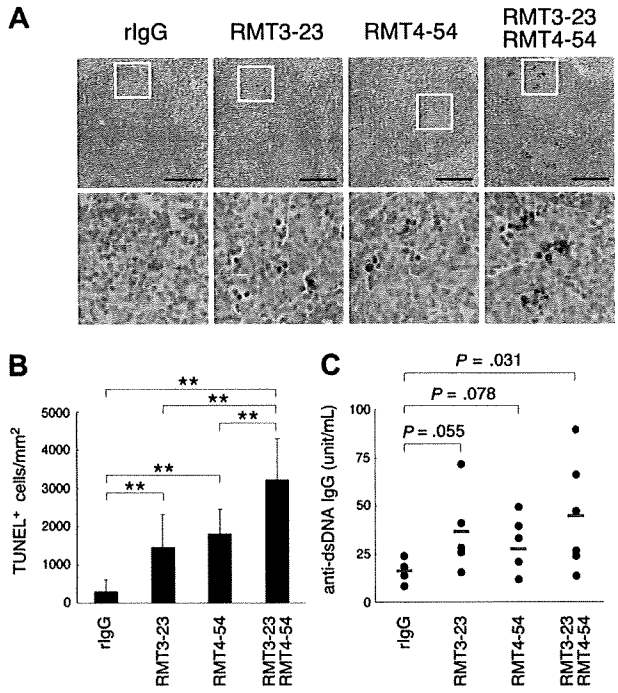

Figure 4. Involvement of Tim-3 in clearance of apoptotic cells in vivo. Mice (n 4-6 per group) were treated with rIgG, RMT3-23, and/or RMT4-54 (200 g each per mouse) twice a week for 4 weeks. (A) Apoptotic cells in paraffin-embedded spleen sections from these mice were detected by TdT-mediated dUTP nick-end labeling (TUNEL) method. Nuclei were counterstained with hematoxylin. Representative sections (top panels, 20 magnification) were shown. Black bars indicate 100 m. White squares mark the areas shown at a higher magnification (bottom panels, 80). (B) The number of TUNEL-positive cells was counted in at least 10 randomly chosen follicles, represented as columns (**P .01). (C) Anti-dsDNA antibody levels in serum were determined by ELISA. P values compared with rIgG are shown. Similar results were obtained in 2 independent experiments.

a previous report.[8] Neither Tim-1 nor Tim-2 was expressed on both types of macrophages (Figure 3A). This result prompted us to investigate whether these different types of macrophages use different Tim molecules to recognize apoptotic cells. As shown in Figure 3B, PRMs efficiently phagocytosed apoptotic cells, and this was significantly inhibited by RMT4-54, but not by RMT3-23. In contrast, phagocytosis of apoptotic cells by PEMs was significantly inhibited by RMT3-23, but not RMT4-54. These results suggest that although these macrophage subsets use MerTK and MFG-E8 to recognize and internalize apoptotic cells,[5,6,32] Tim-3 and Tim-4 also play a role in this process by PEMs and PRMs, respectively. Moreover, we used a mouse sterile peritonitis model to examine whether Tim-3 participates in the phagocytosis in vivo. As shown in Figure 3C, RMT3-23, but not RMT4-54, significantly inhibited the phagocytosis of apoptotic cells by peritoneal macrophages, suggesting that Tim-3 contributes to the phagocytosis of apoptotic cells in vivo.

Tim-3 is crucial for clearance of apoptotic cells in vivo

To evaluate the physiological role of Tim-3 and Tim-4 in vivo, we intraperitoneally injected RMT3-23 and/or RMT4-54 into C57BL/6 mice twice a week for 4 weeks, and stained apoptotic cells in various organs by terminal deoxynucleotidyl transferase–mediated deoxyuridine triphosphate nick-end labeling (TUNEL) method. In spleen follicles, treatment with either RMT3-23 or RMT4-54 significantly increased TUNEL cells, and a remarkable increase was observed with the combination treatment (Figure 4A,B), whereas the administration of these mAbs did not increase the number of TUNEL cells in the liver, pancreas, or brain (not shown).

It has been reported that an impairment of clearance of apoptotic cells induces autoantibody production.[5,33,34] Thus, we next measured serum level of autoantibodies in these mice. Consistent with a recent report,[8] blocking of Tim-4 by RMT4-54 induced anti-dsDNA antibodies (Figure 4C). We found that serum level of anti-dsDNA antibodies was also increased by RMT3-23 (Figure 4C). These results suggest that Tim-3 as well as Tim-4 participates in the clearance of apoptotic cells in vivo, and that the disabling of this system leads to autoantibody production.

Tim-3 mediates phagocytosis of apoptotic cells and cross-presentation by CD8 DCs in vitro

Because Tim-3 is involved in the clearance of apoptotic cells in not only inflammatory state (Figure 3C) but also steady state (Figure 4) in vivo, we further addressed the Tim-3 expression on several types of naive cells, and found that Tim-3 was highly expressed on peripheral blood monocytes and splenic DCs (Figure S3). Moreover, we noticed that the expression of Tim-3 on splenic CD8 DCs was approximately 3-fold higher than that on CD8 DCs (Figure 5A,B). Several groups have demonstrated that, in mouse spleen, CD8 DCs are uniquely able to recognize apoptotic cells, however, the receptor for apoptotic cells remains to be identified.[16-18] These reports prompted us to address whether Tim-3 plays a role for the recognition of apoptotic cells by this DC subset. Consistent with previous reports,[16,35] we observed that CD8 DCs recognized apoptotic cells more efficiently than CD8 DCs (Figure 5C). Interestingly, masking of Tim-3 by RMT3-23 inhibited approximately 50% recognition of apoptotic cells by CD8 DCs (Figure 5C,D), suggesting that CD8 DCs use Tim-3 to efficiently recognize apoptotic cells. Confocal microscopy revealed that, although Tim-3 is largely expressed at cell surface of naive CD8 DCs (Figure 5E left panel), upon recognition of apoptotic cells Tim-3 is recruited to the site of apoptotic cell apposition with the membrane (Figure 5E right panel), suggesting that Tim-3 mediates internalization of apoptotic cells by CD8 DCs.

Because CD8 DC is the splenic DC subset that plays a crucial role in cross-presentation,[15] we next performed cross-presentation study using OT-I T cells specific for $OVA_{257-264}$/H-$2K^b$. Consistent with previous reports,[15,16] we confirmed that CD8 DCs cultured with OVA-loaded, but not BSA-loaded, apoptotic cells could efficiently induce OT-I CD8 T-cell proliferation, and that OT-I cells did not directly respond to OVA-loaded apoptotic cells (Figure S4). Then, we investigated the requirement of Tim-3 for this cross-presentation. As shown in Figure 6A, we observed that CD8 DCs induced OT-I T-cell proliferation more vigorously than CD8 DCs, and that inhibition of the phagocytosis by RMT3-23 significantly abrogated the CD8 DC-induced OT-I cell proliferation. Moreover, we observed a remarkable reduction in IFN- production by RMT3-23 (Figure 6B), whereas both DC subsets loaded with $OVA_{257-264}$ peptides equally activated OT-I T cells, irrespective of masking Tim-3 by RMT3-23. Although splenic DCs express Tim-4 at low level, RMT4-54 did not inhibit the phagocytosis of apoptotic cells and the cross-presentation in vitro (Figures 5,6).

Tim-3 is crucial for phagocytosis of apoptotic cells and cross-presentation in vivo

We further addressed the contribution of Tim-3 to the phagocytosis of apoptotic cells and cross-presentation by CD8 DCs in vivo. It has been reported that intravenously injected apoptotic cells are taken up mainly by CD8 DCs in mouse spleen.[16,35] Consistently,

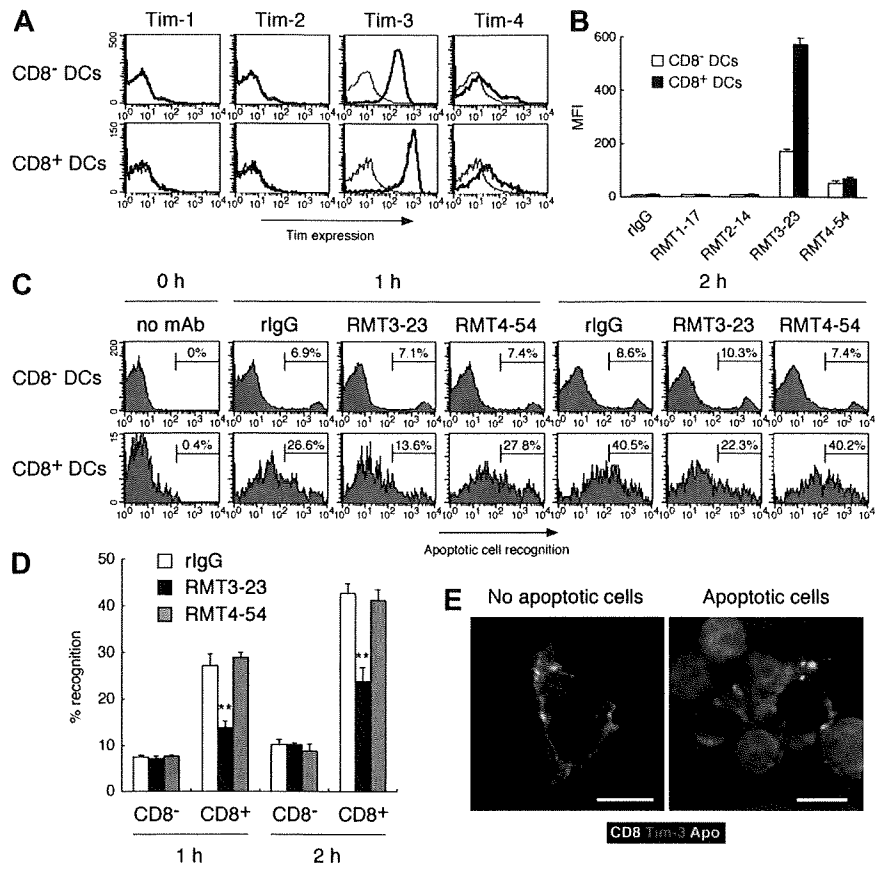

Figure 5. Tim-3 mediates phagocytosis of apoptotic cells by CD8 DCs. (A) Low-density splenocytes were stained with biotinylated control rIgG2a (thin histograms), RMT1-17, RMT2-14, RMT3-23, or RMT4-54 (thick histograms), followed by PE-avidin, FITC–anti-CD11c mAb, and APC–anti-CD8 mAb; then Tim expression on CD8 CD11c or CD8 CD11c cells was analyzed by flow cytometry. The average of mean fluorescence intensity (MFI) SD of triplicates is represented in panel B. (C) Purified splenic CD11c cells prestained with APC–anti-CD8 mAb were treated with rIgG, RMT3-23, or RMT4-54, and then cultured with TAMRA-labeled apoptotic cells at 37°C. After the indicated time period, cells were stained with FITC–anti-CD11c mAb, and percentage recognition of TAMRA-labeled apoptotic cells by CD8 CD11c or CD8 CD11c cells was quantified by flow cytometry. Columns represent mean SD of triplicates in panel D (**P .01 compared with rIgG). (E) (Left panel) Purified splenic CD11c cells were stained with Alexa 647–anti-CD8 mAb and Alexa 594–RMT3-23. (Right panel) Purified splenic CD11c cells prestained with Alexa 647–anti-CD8 mAb were cultured with CFSE-labeled apoptotic cells for 60 minutes at 37°C, and then cells were stained with Alexa 594–RMT3-23. Cells were analyzed by confocal microscopy. White bars indicate 5 m. Similar results were obtained in 3 (A-D) or 2 (E) independent experiments.

we also observed that CD8 DCs efficiently recognized CFSE-labeled apoptotic cells 1 hour after intravenous injection (Figure 7A,B). Interestingly, the recognition was significantly abrogated by RMT3-23. To rule out the possibility that binding of RMT3-23 to FcR on DCs might affect phagocytosis of apoptotic cells, we pretreated mice with anti-FcR (2.4G2). As shown in Figure S5C, 2.4G2 did not affect the blocking activity of RMT3-23. Moreover, we prepared F(ab)$_2$ fragments of RMT3-23, and observed that the F(ab)$_2$ fragments did not lose the blocking effect (Figure S5), indicating that the blocking effect of RMT3-23 is not mediated through FcRs. These results suggest that Tim-3 is crucial for the recognition of apoptotic cells by CD8 DCs in vivo.

To study cross-presentation of apoptotic cell–associated antigens in vivo, we transferred CFSE-labeled OT-I T cells into C57BL/6 mice, and then 1 day later, we primed these mice with OVA-loaded dying splenocytes. Two days after the priming, we observed that OT-I cells proliferated vigorously in spleen (Figure 7C,D), although OT-I cells did not proliferate in unprimed mouse spleen, indicating that dying cell-associated OVA antigens were taken up by splenic CD8 DCs and cross-presented to OT-I cells. Consistent with a crucial role of Tim-3 for the uptake of apoptotic cells by CD8 DCs (Figure 7A,B), the proliferation of OT-I cells was also significantly reduced by RMT3-23, but not RMT4-54 (Figure 7C,D). These results suggest that Tim-3 plays a crucial role in phagocytosis of apoptotic cells and subsequent cross-presentation by CD8 DCs in vivo.

Discussion

Phagocytes such as macrophages and DCs efficiently recognize and engulf apoptotic cells to maintain the peripheral tolerance. In this study, we demonstrate that Tim-3 mediates phagocytosis of apoptotic cells by PEMs and CD8 DCs, and that disabling of the Tim-3 function in vivo induces autoantibody production. Likewise, several studies have shown that impairment of the clearance of apoptotic cells causes autoantibody production,[5,8,34] however, the mechanism for the elicited immune response to dying cells remains to be elucidated. As the possible explanation, delay or impairment of clearance of apoptotic cells by macrophages causes secondary necrotic cells releasing intracellular contents, which could be endogenous "danger signal" activating immune system.[1] However, chronic administration of apoptotic thymocytes to syngeneic mice induces more remarkable level of autoantibody production than that of the same dose of nonapoptotic cell lysate,[36] suggesting that autoantibody production in response to dying cells could not be explained simply by the exposure of the intracellular contents. It has also been reported that, in mice, CD8 DC subset is unique in its ability to recognize apoptotic cells and cross-present dying cell-associated antigens.[15,16] It is considered that, in steady state, cross-presentation of dying cell-associated self-antigens by CD8 DCs induces autoreactive CD8 T-cell proliferation abortively, subsequently resulting in their deletion, which is important to maintain peripheral tolerance.[10,13,14] Taken together, Tim-3–mediated phagocytosis of apoptotic cells by CD8 DCs may be linked to peripheral tolerance, and a loss of Tim-3 function in DCs may exacerbate autoimmunity. Consistent with this hypothesis, we and others have reported that Tim-3 negatively regulates Th1-mediated inflammatory diseases such as EAE, type I diabetes, and aGVHD, and promotes tolerance induction.[21-23]

Alternatively, however, upon being activated by anti-CD40 mAb, endogenous danger signals such as heat shock proteins and uric acid, or pathogen-associated molecular patterns (PAMPs) such as LPS and CpG, DCs turn to cross-prime CD8 T cells to generate

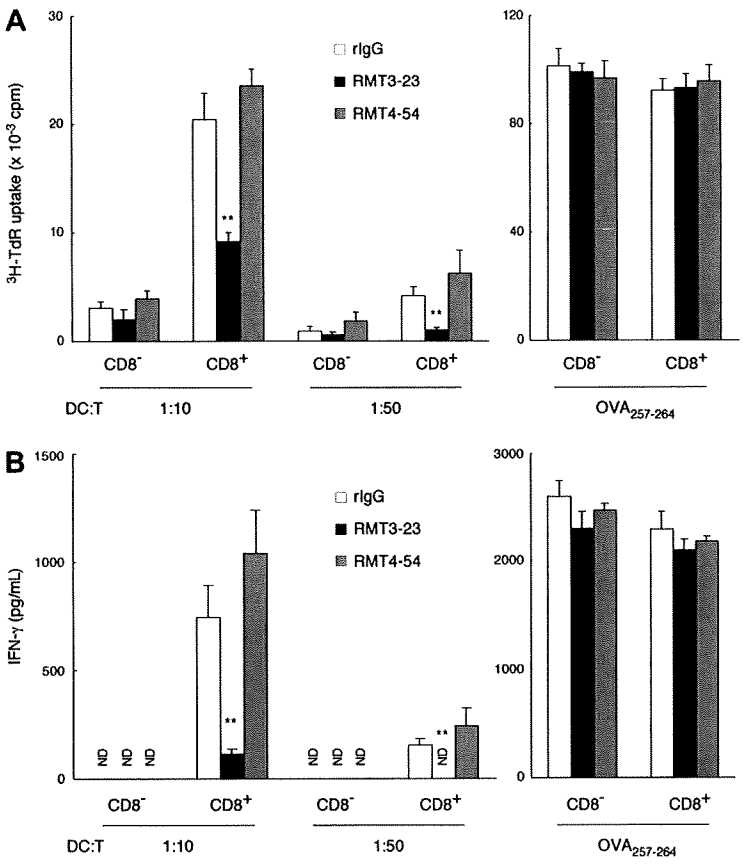

Figure 6. Tim-3–mediated phagocytosis of apoptotic cells is crucial for the cross-presentation by CD8 DCs. (A) Purified CD8 CD11c or CD8 CD11c splenic DCs were pretreated with rIgG (white histograms), RMT3-23 (black histograms), or RMT4-54 (gray histograms) and then cultured with OVA-loaded apoptotic cells. After 2 hours, both DC subsets were purified again to remove dead cells, and then cocultured with OT-I CD8 T cells at the indicated ratio. For the direct presentation, both DC subsets preincubated with $OVA_{257-264}$ peptide (1 nM) in the presence of rIgG, RMT3-23, or RMT4-54 were cocultured with OT-I CD8 T cells at a 1:10 (DC/T) ratio. [^{3}H]thymidine (^{3}H-TdR) uptake was measured at 48 to 60 hours. (B) Production of IFN- in the culture supernatant at 48 hours after addition of OT-I CD8 T cells was measured by ELISA. Columns represent mean SD of triplicates (**P .01 compared with rIgG). ND indicates not detectable. Similar results were obtained in 3 independent experiments (A,B).

effector cells.[10,12] Given that Tim-3 is crucial for IFN- production in cross-presentation and that Tim-3 is expressed on sterile inflammatory macrophages, Tim-3 may promote induction of effector CD8 T-cell proliferation and functional memory under pathological conditions. Indeed, Anderson et al have recently reported that Tim-3 expressed on DCs exacerbates a Th1-type autoimmune disease EAE.[25] Although Tim-3 has been reported to have multiple functions,[21-23] it would be important to further address whether this novel function of Tim-3 is linked to immune tolerance or activation under pathological conditions.

It remains unclear why CD8 DCs are not able to engulf apoptotic cells efficiently, although this DC subset expresses Tim-3. One possibility is that the phagocytic activity may be determined by relative expression level of receptors for "eat-me" signals and "don't eat-me" signals. Although we observed that expression level of Tim-3 on CD8 DCs is approximately 3-fold higher than that on CD8 DCs, it has been reported that signal-regulatory protein (SIRP) , a receptor for "don't eat-me" signal,[37] is much more highly expressed on CD8 DCs than CD8 DCs.[38] Taken together, a high expression of Tim-3 may be required for the phagocytosis by DCs, and/or SIRP may neutralize Tim-3 function on CD8 DCs. Moreover, phagocytic activity of each cell type may be determined not only by expression level of the phagocytic receptor, but also cell-intrinsic phagocytic machinery such as cytoskeletal architecture. Indeed, Tim-3 as well as Tim-1 is expressed on activated T cells,[24,39] but these T cells are not able to recognize apoptotic cells.

In this study, ectopic expression of Tim-3 enabled HEK293T cells to engulf whole apoptotic cells. However, Miyanishi et al could not observe the phagocytic activity of Tim-3 expressed on NIH3T3 cells based on their engulfment assay, which quantified nuclear DNA degradation of apoptotic cells engulfed by NIH3T3 expressing Tim-3 and DNase II.[8] To address this discrepancy, we also generated NIH3T3 cells expressing Tim-3, and did not observe the ability of Tim-3 to mediate engulfment of whole apoptotic cells, although we did observe the ability of Tim-3 to incorporate CFSE-labeled apoptotic cell debris (Figure S6). The reason why Tim-3 expressed on NIH3T3 cells is not able to efficiently phagocytose apoptotic cells remains to be elucidated. We cannot rule out the possibility that Tim-3 may recognize apoptotic cells in cooperation with some coreceptor, which may be expressed on HEK293T cells, macrophages, and CD8 DCs, but not NIH3T3 cells or CD8 DCs. Likewise, it has been reported that although gene targeting of MerTK receptor results in remarkable defect of phagocytosis of apoptotic cells by macrophages,[5] the receptor requires coexpression of $_V$ $_5$ integrin to enable NIH3T3 cells to recognize apoptotic cells.[40] Although we did observe PS binding of Tim-3 by solid-phase ELISA, Miyanishi et al failed to observe this by PIP–strip binding assay.[8] This discrepancy is probably due to a difference in assay sensitivity. Given that the affinity of Tim-3 to PS is much lower than that of Tim-4, Tim-3 might bind not only PS but also some other ligand to phagocytose apoptotic cells. Further studies are needed to elucidate the complexity of phagocytosis.

We show here a crucial role of Tim-3 for clearance of apoptotic cells in vivo and differential expression profile of phagocytic Tim molecules, suggesting that the pathophysiological roles of each Tim molecule appear to be different. Because Tim-1 is expressed on epithelial cells but not professional phagocytes, Tim-1 may contribute to remodeling of injured epithelia.[9] Tim-4 is highly expressed on PRMs, and contributes to the phagocytosis of apoptotic cells during physiological tissue turnover.[8] Our findings highlight Tim-3 as the phagocytic receptor responsible for cross-presentation by CD8 DCs. This novel function of Tim-3 opens the door to new therapeutic approaches to combat infections, cancers, and autoimmune diseases.

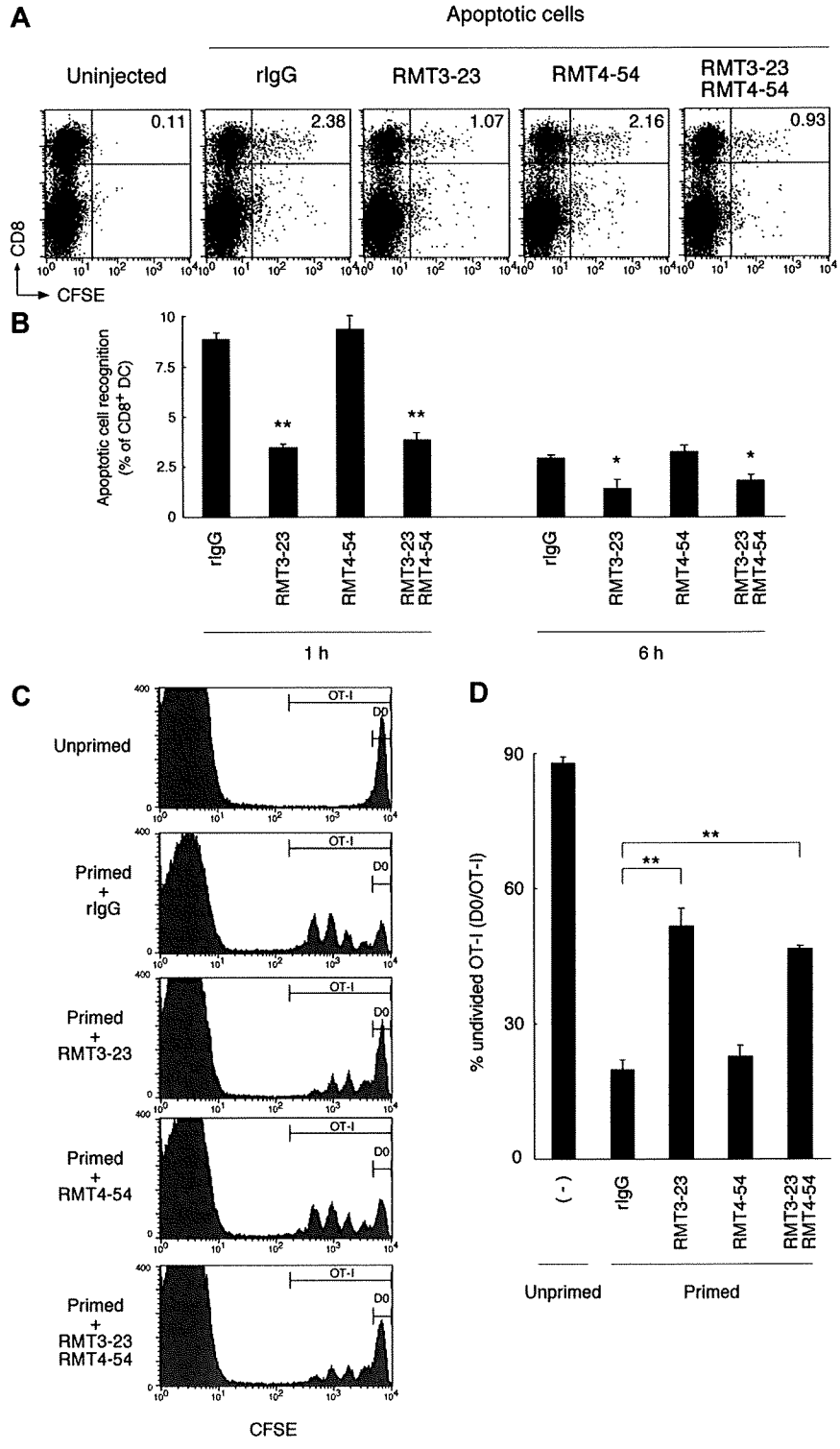

Figure 7. Tim-3 is crucial for the phagocytosis of apoptotic cells and cross-presentation in vivo. (A) Mice (n 3 per group) were intravenously injected with the indicated mAb (200 g each per head), and then 2 hours later with CFSE-labeled apoptotic splenocytes (2 10^7 per head). One hour later, collagenase-digested splenocytes were harvested, and recognition of CFSE-labeled apoptotic cells by splenic CD11c cells was analyzed by flow cytometry. Numbers indicate percentage of cells in top right quadrants. (B) Collagenase-digested splenocytes were harvested from mice treated as described in panel A at indicated time points, and recognition of apoptotic cells by splenic CD8 DCs was analyzed by flow cytometry. Percentage recognition of CFSE-labeled apoptotic cells by CD8 DCs (percentage CFSE CD8 CD11c cells/percentage CD8 CD11c cells 100) was calculated. Columns represent mean SD of triplicates (*P .05; **P .01 compared with rIgG). Similar results were obtained in 3 independent experiments. (C) CFSE-labeled OT-I CD8 T cells (2 10^6 per head) were intravenously transferred into B6 mice (n 3 per group). The next day, mice were intravenously injected with the indicated mAb (200 g each per head), and then 2 hours later primed with OVA-loaded apoptotic cells (10^7 per head). Two days later, whole splenocytes were harvested, and CFSE intensity of CD8 V 2 OT-I cells was analyzed by flow cytometry. Percentage of undivided cells in total OT-I cells (D0 per OT-I in C) was calculated, and mean SD of triplicates was shown in panel D (**P .01 compared with rIgG). Similar results were obtained in 3 independent experiments.

Acknowledgments

We thank Drs William R. Heath for OT-I mice, Sachiko Hirose for aged (NZB NZW) F1 mice serum, and Toshio Kitamura for pMXs-IRES-puro vector. We also thank Dr Tamami Sakanishi for cell sorting.

This work was supported by the Grants-in-Aid for Scientific Research from the Japanese Ministry of Education, Culture, Sports, Science and Technology (Tokyo, Japan), and by a grant from "High-Tech Research Center" Project for Private Universities: matching fund subsidy from the Ministry of Education, Culture, Sports, Science and Technology (Tokyo, Japan).

Authorship

Contribution: M.N. designed and performed experiments; H.A. provided vital reagents; H.A., Y.K., and M.H. discussed experimental strategy and performed experiments; K.T. designed and discussed experimental strategy; M.A., H.Y., and K.O. supervised

experiments and discussed the experimental strategy; M.N. wrote the paper; and K.T. and H.Y. edited the paper.

Conflict-of-interest disclosure: The authors declare no competing financial interests.

Correspondence: Masafumi Nakayama, Department of Immunology, Juntendo University School of Medicine, 2-1-1 Hongo, Bunkyo-ku, Tokyo 113-8421, Japan; e-mail: nakayama@juntendo.ac.jp.

References

1. Savill J, Dransfield I, Gregory C, Haslett C. A blast from the past: clearance of apoptotic cells regulates immune responses. Nat Rev Immunol. 2002;2:965-975.
2. Henson PM, Hume DA. Apoptotic cell removal in development and tissue homeostasis. Trends Immunol. 2006;27:244-250.
3. Cohen JJ, Duke RC, Fadok VA, Sellins KS. Apoptosis and programmed cell death in immunity. Annu Rev Immunol. 1992;10:267-293.
4. Ravichandran KS, Lorenz U. Engulfment of apoptotic cells: signals for a good meal. Nat Rev Immunol. 2007;7:964-974.
5. Scott RS, McMahon EJ, Pop SM, et al. Phagocytosis and clearance of apoptotic cells is mediated by MER. Nature. 2001;411:207-211.
6. Hanayama R, Tanaka M, Miwa K, Shinohara A, Iwamatsu A, Nagata S. Identification of a factor that links apoptotic cells to phagocytes. Nature. 2002;417:182-187.
7. Park D, Tosello-Trampont AC, Elliott MR, et al. BAI1 is an engulfment receptor for apoptotic cells upstream of the ELMO/Dock180/Rac module. Nature. 2007;450:430-434.
8. Miyanishi M, Tada K, Koike M, Uchiyama Y, Kitamura T, Nagata S. Identification of Tim4 as a phosphatidylserine receptor. Nature. 2007;450:435-439.
9. Kobayashi N, Karisola P, Pena-Cruz V, et al. TIM-1 and TIM-4 glycoproteins bind phosphatidylserine and mediate uptake of apoptotic cells. Immunity. 2007;27:927-940.
10. Heath WR, Belz GT, Behrens GM, et al. Cross-presentation, dendritic cell subsets, and the generation of immunity to cellular antigens. Immunol Rev. 2004;199:9-26.
11. Kurts C, Kosaka H, Carbone FR, Miller JF, Heath WR. Class I-restricted cross-presentation of exogenous self-antigens leads to deletion of autoreactive CD8( ) T cells. J Exp Med. 1997;186:239-245.
12. Liu K, Iyoda T, Saternus M, Kimura Y, Inaba K, Steinman RM. Immune tolerance after delivery of dying cells to dendritic cells in situ. J Exp Med. 2002;196:1091-1097.
13. Redmond WL, Sherman LA. Peripheral tolerance of CD8 T lymphocytes. Immunity. 2005;22:275-284.
14. Luckashenak N, Schroeder S, Endt K, et al. Constitutive crosspresentation of tissue antigens by dendritic cells controls CD8 T cell tolerance in vivo. Immunity. 2008;28:521-532.
15. den Haan JM, Lehar SM, Bevan MJ. CD8( ) but not CD8( ) dendritic cells cross-prime cytotoxic T cells in vivo. J Exp Med. 2000;192:1685-1696.
16. Iyoda T, Shimoyama S, Liu K, et al. The CD8 dendritic cell subset selectively endocytoses dying cells in culture and in vivo. J Exp Med. 2002;195:1289-1302.
17. Schulz O, Pennington DJ, Hodivala-Dilke K, Febbraio M, Reis e Sousa C. CD36 or alphavbeta3 and alphavbeta5 integrins are not essential for MHC class I cross-presentation of cell-associated antigen by CD8 alpha murine dendritic cells. J Immunol. 2002;168:6057-6065.
18. Belz GT, Vremec D, Febbraio M, et al. CD36 is differentially expressed by CD8 splenic dendritic cells but is not required for cross-presentation in vivo. J Immunol. 2002;168:6066-6070.
19. Monney L, Sabatos CA, Gaglia JL, et al. Th1-specific cell surface protein Tim-3 regulates macrophage activation and severity of an autoimmune disease. Nature. 2002;415:536-541.
20. Anderson AC, Anderson DE. TIM-3 in autoimmunity. Curr Opin Immunol. 2006;18:665-669.
21. Sabatos CA, Chakravarti S, Cha E, et al. Interaction of Tim-3 and Tim-3 ligand regulates T helper type 1 responses and induction of peripheral tolerance. Nat Immunol. 2003;4:1102-1110.
22. Sánchez-Fueyo A, Tian J, Picarella D, et al. Tim-3 inhibits T helper type 1-mediated auto- and alloimmune responses and promotes immunological tolerance. Nat Immunol. 2003;4:1093-1101.
23. Oikawa T, Kamimura Y, Akiba H, et al. Preferential involvement of Tim-3 in the regulation of hepatic CD8 T cells in murine acute graft-versus-host disease. J Immunol. 2006;177:4281-4287.
24. Zhu C, Anderson AC, Schubart A, et al. The Tim-3 ligand galectin-9 negatively regulates T helper type 1 immunity. Nat Immunol. 2005;6:1245-1252.
25. Anderson AC, Anderson DE, Bregoli L, et al. Promotion of tissue inflammation by the immune receptor Tim-3 expressed on innate immune cells. Science. 2007;318:1141-1143.
26. Xiu Y, Nakamura K, Abe M, et al. Transcriptional regulation of Fcgr2b gene by polymorphic promoter region and its contribution to humoral immune responses. J Immunol. 2002;169:4340-4346.
27. Li M, Davey GM, Sutherland RM, et al. Cell-associated ovalbumin is cross-presented much more efficiently than soluble ovalbumin in vivo. J Immunol. 2001;166:6099-6103.
28. Peiser L, Gough PJ, Kodama T, Gordon S. Macrophage class A scavenger receptor-mediated phagocytosis of Escherichia coli: role of cell heterogeneity, microbial strain, and culture conditions in vitro. Infect Immun. 2000;68:1953-1963.
29. Nakayama M, Underhill DM, Petersen TW, et al. Paired Ig-like receptors bind to bacteria and shape TLR-mediated cytokine production. J Immunol. 2007;178:4250-4259.
30. Santiago C, Ballesteros A, Martinez-Munoz L, et al. Structures of T cell immunoglobulin mucin protein 4 show a metal-Ion-dependent ligand binding site where phosphatidylserine binds. Immunity. 2007;27:941-951.
31. Cao E, Zang X, Ramagopal UA, et al. T cell immunoglobulin mucin-3 crystal structure reveals a galectin-9-independent ligand-binding surface. Immunity. 2007;26:311-321.
32. Hu B, Jennings JH, Sonstein J, et al. Resident murine alveolar and peritoneal macrophages differ in adhesion of apoptotic thymocytes. Am J Respir Cell Mol Biol. 2004;30:687-693.
33. Asano K, Miwa M, Miwa K, et al. Masking of phosphatidylserine inhibits apoptotic cell engulfment and induces autoantibody production in mice. J Exp Med. 2004;200:459-467.
34. Hanayama R, Tanaka M, Miyasaka K, et al. Autoimmune disease and impaired uptake of apoptotic cells in MFG-E8-deficient mice. Science. 2004;304:1147-1150.
35. Schnorrer P, Behrens GM, Wilson NS, et al. The dominant role of CD8 dendritic cells in cross-presentation is not dictated by antigen capture. Proc Natl Acad Sci U S A. 2006;103:10729-10734.
36. Mevorach D, Zhou JL, Song X, Elkon KB. Systemic exposure to irradiated apoptotic cells induces autoantibody production. J Exp Med. 1998;188:387-392.
37. Gardai SJ, McPhillips KA, Frasch SC, et al. Cell-surface calreticulin initiates clearance of viable or apoptotic cells through trans-activation of LRP on the phagocyte. Cell. 2005;123:321-334.
38. Lahoud MH, Proietto AI, Gartlan KH, et al. Signal regulatory protein molecules are differentially expressed by CD8- dendritic cells. J Immunol. 2006;177:372-382.
39. de Souza AJ, Oriss TB, O'Malley KJ, Ray A, Kane LP. T cell Ig and mucin 1 (TIM-1) is expressed on in vivo-activated T cells and provides a costimulatory signal for T cell activation. Proc Natl Acad Sci U S A. 2005;102:17113-17118.
40. Wu Y, Singh S, Georgescu MM, Birge RB. A role for Mer tyrosine kinase in alphavbeta5 integrin-mediated phagocytosis of apoptotic cells. J Cell Sci. 2005;118:539-553.

DOI:10.1111/j.1600-0625.2007.00618.x
www.blackwellpublishing.com/EXD

Original Article

Antimelanogenesis effect of Tunisian herb *Thymelaea hirsuta* extract on B16 murine melanoma cells

Mitsuko Kawano[1], Kyoko Matsuyama[1], Yusaku Miyamae[2], Hiroshi Shinmoto[3], Mohamed Elyes Kchouk[4], Takahiro Morio[1], Hideyuki Shigemori[2] and Hiroko Isoda[1]

[1]Alliance for Research on North Africa, University of Tsukuba, Tsukuba, Ibaraki, Japan;
[2]Graduate School of Life and Environmental Sciences, University of Tsukuba, Tsukuba, Ibaraki, Japan;
[3]National Food Research Institute, Tsukuba, Ibaraki, Japan;
[4]Biotechnology Center, Borj Cedria Technopark, Hammam-Lif, Tunisia
Correspondence: Hiroko Isoda, PhD, Alliance for Research on North Africa (ARENA), University of Tsukuba, 1-1-1 Tennodai, Tsukuba, Ibaraki 305-8572, Japan, Tel.:+81 29 853 5775, Fax: +81 29 853 5776, e-mail: isoda@sakura.cc.tsukuba.ac.jp

Accepted for publication 11 July 2007

Abstract: Skin pigmentation is the result of melanogenesis that occurs in melanocytes and/or melanoma cells. Although melanogenesis is necessary for the prevention of DNA damage and cancer caused by UV irradiation, excessive accumulation of melanin can also cause melanoma. Thus, we focused on the antimelanogenesis effect of an extract from *Thymelaea hirsuta*, a Tunisian herb. Murine melanoma B16 cells were treated with *T. hirsuta* extract, and then cell viability and synthesized melanin content were measured. We found that the *T. hirsuta* extract decreased the synthesized melanin content in B16 cells without cytotoxicity. Tyrosinase is a key enzyme of melanogenesis and extracellular signal-regulated kinase (ERK)-1/2 phosphorylation is known to be related to melanogenesis inhibition. To clarify its mechanism, we also determined ERK1/2 phosphorylation and tyrosinase expression level. ERK1/2 was immediately phosphorylated in cells just after treatment with the extract. The tyrosinase expression was inhibited after 24 h of stimulation with the extract. The *T. hirsuta* extract was fractionated, and we found that one fraction considerably decreased the melanin synthesis in B16 cells and that this fraction contains daphnanes as the main component. This indicates that our findings might be attributable to daphnanes.

Key words: antimelanogenesis – B16 melanoma – tyrosinase – ERK1/2 – *Thymelaea hirsuta*

Please cite this paper as: Antimelanogenesis effect of Tunisian herb *Thymelaea hirsuta* extract on B16 murine melanoma cells. Experimental Dermatology 2007; 16: 977–984.

Introduction

In mammals, melanin is synthesized in the melanosomes of melanocytes. Its synthesis is regulated by melanogenic enzymes such as tyrosine, tyrosinase-related protein 1 (TRP-1) and tyrosinase-related protein 2 (TRP-2) (1–3). Tyrosinase is a copper enzyme and a key enzyme in the process of melanogenesis from L-tyrosine to 3,4-dihydroxyphenylalanine (DOPA), and then it catalyses the oxidation of DOPA into DOPA quinine. TRP-2, which functions as DOPA-chrome tautomerase, catalyses the rearrangement of DOPA-chrome into 5,6-dihydroxyindole-2-carboxylic acid (DHICA), and TRP-1 oxidizes DHICA into a carboxylated indole-quinone. The stimulation of tyrosinase activity is thus related to melanogenesis.

Thymelaea is a genus comprising about 30 species of evergreen shrubs under the flowering plant family *Thymelaeaceae*, which is native to the Canary Island, the Mediterranean region, north of central Europe, and east of central Asia. In this report, we focused on *T. hirsuta*, which is native to North Africa. In the Republic of Tunisia, this plant has been used traditionally as an antiseptic and for the treatment of hypertension. However, its traditional medicinal uses are not based on scientific research or investigation, and other effects have not been clarified.

The Republic of Tunisia is located in North Africa, and its north side faces the Mediterranean Sea while its south side leads to the Sahara. Between the Mediterranean Sea and the Sahara, the distance is only 100–350 km. This means that the dryness gradient is very high and plants in this area might have some antistress factors in their system, because plants that have evolved in this area could not have survived without accumulating these factors. Thus, we focused on this area and screened Tunisian medicinal plants for unique and new biological activities. We decided to evaluate the biological activity of *T. hirsuta* extract in relation to the maintenance of skin homeostasis, particularly for melanogenesis as a new activity.

Recently, the antimelanogenesis and/or melanogenesis stimulation effect by plant extracts have been reported (4–13). Many of these articles focused only on tyrosinase activity and expression levels. In this study, we focused on not only tyrosinase expression, but also on the intracellular signal transduction cascade. The antimelanogenesis effect of the *T. hirsuta* extract on cultured murine B16 melanoma cells was investigated.

Materials and methods

Extraction of *T. hirsuta*

Aerial leaves of *T. hirsuta* (10 g) were extracted with 70% EtOH (100 ml) for 1–2 weeks at room temperature. After extraction, the extract was filter-sterilized using a 0.45 μm pore size filter (Millipore, Billerica, MA, USA) and then stored at −80°C until use.

Cells and cell culture

Mouse B16 melanoma cells (4A-5) were purchased from the Riken Cell Bank (Tsukuba, Japan). B16 mouse melanoma cells were maintained as a monolayer culture in Dulbecco's modified Eagle's medium (Nissui, Tokyo, Japan) supplemented with 10% fetal bovine serum (Sigma, St Louis, MO, USA), 4 mM L-glutamine (Sigma), 50 units/ml penicillin and 50 μg/ml streptomycin (Cambrex, East Rutherford, NJ, USA) at 37°C in a humidified atmosphere of 5% CO_2.

Measurement of melanin content

The melanin content was measured by a modification of the method of Hosoi et al. (14). B16 melanoma cells were seeded onto 100-mm dishes at a density of 5×10^5 cells per dish and cultivated by the method described above. After overnight incubation, the medium was replaced with sample-containing medium (200-, 2000- and 20 000-fold dilution or 0.5 μg/ml of sample) and incubated further for 2 days. The medium was then removed, and then the cells were washed twice with phosphate-buffered saline (PBS) and harvested by trypsinization (0.25% trypsin/0.02% EDTA in PBS; Sigma). The harvested cells were pelleted and the cell membrane was dissolved using 0.1% Triton X-100. The synthesized melanin was then purified and precipitated in 10% trichloroacetate. The purified melanin was dissolved by incubation in 8 N NaOH for 2 h at 80°C. The absorbance of the solution was measured at 410 nm and the melanin content was calculated using a standard curve for synthetic melanin.

Western blotting

B16 melanoma cells were seeded onto 100-mm dishes at a density of 3×10^6 cells per dish and cultivated by the method described above. After overnight incubation, the medium was replaced with 300-fold-diluted sample-containing medium followed by incubation for 0.5, 1, 2, 5, 24 or 48 h. The medium was then removed, the cells were washed twice with PBS and total protein was extracted using RIPA buffer (Sigma) according to the manufacturer's instructions. Fifteen micrograms of extracted protein sample was resolved by 12% (for activated ERK1/2 and ERK2) or 10% (for tyrosinase) sodium dodecyl sulphate-polyacrylamide gel electrophoresis (SDS-PAGE), transferred to nitrocellulose membrane, and blotted with anti-activated ERK1/2 monoclonal antibody (Sigma; 1:1785 dilution), anti-ERK2 monoclonal antibody (Sigma; 1:660 dilution), and anti-tyrosinase polyclonal antibody (Santa Cruz Biotechnology, Inc., Santa Cruz, CA, USA; 1:200 dilution). The signal was visualized using Immobilon Western Chemiluminescent HRP Substrate (Millipore), after reaction with labelled anti-mouse IgG_1 antibody (for activated ERK1/2 and ERK1/2; Zymed Laboratories Inc., San Francisco, CA, USA; 1:1000 dilution) or HRP-labelled anti-rabbit IgG antibody (for tyrosinase; Santa Cruz Biotechnology, Inc.; 1:2000 dilution). As a loading control for the assay on tyrosinase expression, the SDS-PAGE gels were stained with Coomassie brilliant blue (CBB), as follows. After SDS-PAGE, the gels were fixed twice for 15 min each time with a fixation solution containing 40% (v/v) acetic acid and 50% (v/v) MeOH. The fixed gels were then stained with CBB (Wako, Osaka, Japan).

Cell viability assay

Cell viability was determined with Guava PCA (GE Healthcare, UK Ltd, Buckinghamshire, UK) using the ViaCount program for analysis. B16 murine melanoma cells were seeded onto 100 mm dishes at a density of 5.0×10^5 cells per dish and cultivated by the method described above. After overnight incubation, the medium was replaced with sample-containing medium (200-, 2000- and 20 000-fold dilution) and further incubated for 2 days. After medium removal, the cells were washed twice with PBS and harvested by trypsinization. The harvested cells were resuspended in growth medium and stained with the ViaCount reagent (GE Healthcare, UK Ltd) according to the manufacturer's instructions. The ViaCount reagent differentially stains viable and non-viable cells based on their permeability to the DNA-binding dyes in the reagent. The fluorescence of each dye is resolved operationally, allowing the quantitative assessment of viable and non-viable nucleated cells present in a suspension. The system counts the stained nucleated events, and then uses the forward scatter properties to distinguish free nuclei and cellular debris from cells.

F-actin staining

F-actin polymerization was detected by fluorescent dye staining of B16 cells using phalloidin-rhodamine. B16 murine melanoma cells were subcultured onto four-well chamber slides (Nunc, Rochester, NY, USA) at a density of 4.0×10^4

cells per well. After overnight incubation, the medium was replaced with sample-containing medium (1000-fold dilution) and further incubated for 24 h. After medium removal, the cells were washed with PBS and fixed with 3.7% formaldehyde for 5 min. After fixation, the cells were washed and permeabilized with 0.2% Triton X-100 in PBS for 5 min, and then washed three times. Rhodamine-phalloidin (Cytoskeleton Inc., Denver, CO, USA) was added to the cells at 70 nM for 30 min at room temperature in the dark and the cells were then washed thrice with PBS. Mounting reagent containing DAPI (Vector Laboratories, Inc., Burlingame, CA, USA) was then added and fluorescent signals were then detected and photographed using a Leica DMI-4000B fluorescence microscope and a Leica DFC300FX CCD camera (Leica, Wetzlar, Germany). The images were analysed using the Leica Application Suite (Leica).

Fractionation of *T. hirsuta* extract

Aerial leaves (100 g) of *T. hirsuta* were extracted with MeOH (1.3 l) and evaporated to dryness *in vacuo* at 30°C. The MeOH extract (8.03 g) was then partitioned between EtOAc (500 ml × 3) and H_2O (500 ml). The H_2O-soluble portion was partitioned with BuOH (500 ml × 3). The EtOAc-soluble portion (1.30 g) was fractionated into 17 fractions (*Th*-EtOAc-1–17) using a silica gel column ($\varphi\xi$ 2.2 × 33 cm, hexane/EtOAc, 5:1 → 2:1 → $CHCl_3$/MeOH, 8:1 → 0:100). *Th*-EtOAc-11 was separated into six fractions (*Th*-EtOAc-11-1–6) by a C_{18} Sep-Pak cartridge (MeOH/H_2O, 50:50 → 100:0 → $CHCl_3$/MeOH, 1:6 → 100:0 water).

Extraction and isolation of daphnanes from *T. hirsuta*

Leaves (100 g) of *T. hirsuta* were extracted with MeOH (1.3 l) and evaporated to dryness *in vacuo* at 30°C. The MeOH extract (8.0 g) was then partitioned between EtOAc (500 ml × 3) and H_2O (500 ml). The H_2O-soluble portion was partitioned with BuOH (500 ml × 3). The EtOAc-soluble material (1.30 g) was subjected to a silica gel column (φ 2.2 × 33 cm, hexane/EtOAc, 5:1 → 2:1 → $CHCl_3$/MeOH, 8:1 → 0:100) to afford 17 fractions (*Th*-EtOAc-1–17). *Th*-EtOAc-11 was separated into six fractions (*Th*-EtOAc-11-1–6) by a C_{18} Sep-Pak cartridge (MeOH/H_2O, 50:50 → 100:0 → $CHCl_3$/MeOH, 1:6 → 100:0; Waters, Milford, MA, USA). *Th*-EtOAc-11-3 was purified by reversed-phase C_{18} HPLC [Inertsil ODS3 (1.0 × 25 cm), flow rate 2.0 ml/min; solvent CH_3CN/H_2O (65:35)] to give two daphnane diterpenoids, *Th*-EtOAc-11-3-6 and *Th*-EtOAc-11-3-8.

Structural analysis

^{1}H-NMR spectra were measured and recorded using a Brucker AVANCE 500 spectrometer and EIMS was recorded on an MS-6890.

Th-EtOAc-11-3-6 (genkwadaphnin): EIMS *m/z* 602 (M^+), ^{1}H-NMR ($CDCl_3$, 500 MHz): δ7.60–7.75 (m, aromatic-H), 7.50 (s, 1H), 5.28 (s, 1H), 5.05 (s, 2H), 4.95 (d, J = 2.5 Hz, 1H), 4.25 (s, 1H), 3.90 (m, 1H), 3.85 (d, J = 5.4 Hz, 2H), 3.63 (br s, 1H), 2.63 (q, J = 7.3 Hz, 1H), 1.88 (s, 3H), 1.75 (d, J = 2.6 Hz, 3H), and 0.88 (m, 3H).

Th-EtOAc-11-3-8 (gnidicin): EIMS *m/z* 628 (M^+), ^{1}H-NMR ($CDCl_3$, 500 MHz): δ7.60–7.75 (m, aromatic-H), 7.50 (s, 1-H), 6.37 (d, J = 16.0 Hz, 1H), 5.18 (s, 1H), 5.05 (s, 2H), 4.95 (d, J = 2.5 Hz, 1H), 4.25 (s, 1H), 3.90 (m, 1H), 3.85 (d, J = 5.4 Hz, 2H), 3.63 (br s, 1H), 2.52 (q, J = 7.3 Hz, 1H), 1.88 (s, 3H), 1.75 (d, J = 2.6 Hz, 3H), and 0.88(m, 3H).

Statistics

Differences between means were assessed for significance using the Student's *t*-test.

Results

Inhibitory effect of *T. hirsuta* extract on melanin synthesis in B16 melanoma cells without cytotoxicity

The effect of *T. hirsuta* extract on the melanogenesis of B16 mouse melanoma cells was examined. We observed that B16 mouse melanoma cells treated with *T. hirsuta* extract showed a time-dependent decrease in cytoplasmic accumulation of melanin (Fig. 1a). We quantified the synthesized melanin content per cell and found that the extract inhibited melanin synthesis by more than 50% versus control (Fig. 1b) in a dose-dependent manner, suggesting that the extract can inhibit melanin synthesis in B16 mouse melanoma cells.

To determine the cytotoxicity of *T. hirsuta* extract on B16 murine melanoma cells, we performed the cell viability assay using the Guava ViaCount system. From this assay, we found that the extract is not cytotoxic to B16 murine melanoma cells after 48 h of incubation (Fig. 1b). Observation of the cells treated with the extract using a phase-contrast microscope also showed the absence of cytotoxicity (Fig. 1a).

These results suggest that the extract has antimelanogenesis effect on B16 cells without cytotoxicity. Moreover, cells incubated with the extract for more than 24 h showed the ability to undergo mitosis without melanin accumulation.

Melanogenesis inhibition by *T. hirsuta* extract via MAPK activation

Recently, ERK1/2, a key molecule in the mitogen-activated protein kinase (MAPK) intracellular signal transduction cascade, has been reported to be associated with melanogenesis. The phosphorylation of ERK1/2 contributes to antimelanogenesis. To determine the mechanism of

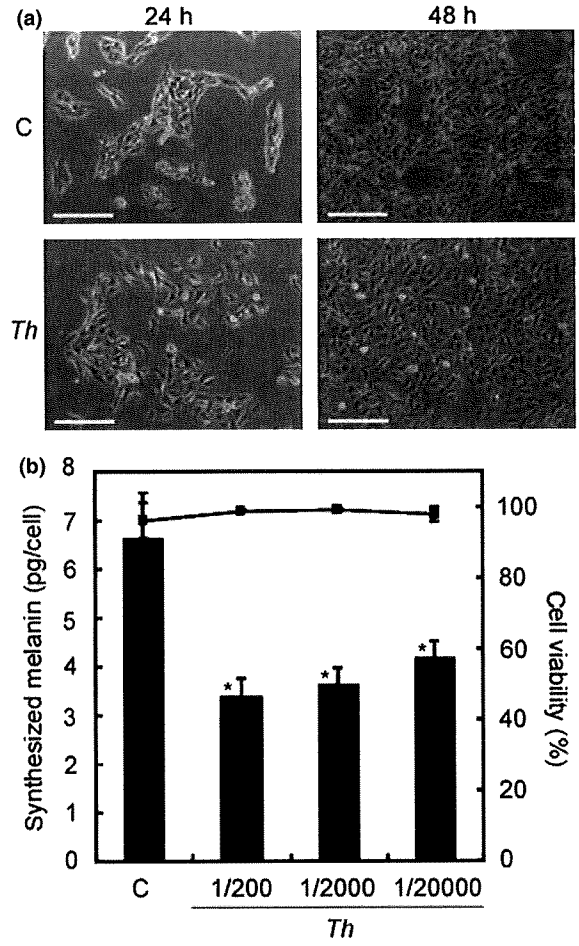

Figure 1. Effect of *Thymelaea hirsuta* extract on melanogenesis in B16 murine melanoma cells. (a) Change in shape of B16 cells treated with *T. hirsuta* extract. B16 cells were seeded at a density of 5×10^5 cells per 100-mm dish. After overnight incubation, the cells were treated with (*Th*, lower panels) or without (C, upper panels) *T. hirsuta* extract at 2000-fold dilution for 24 h (left panels) or 48 h (right panels). All photographs were taken at 100× magnification and each bar represents 200 μm. (b) Synthesized melanin content and cell viability of B16 murine melanoma cells treated with *T. hirsuta* extract. B16 cells were seeded at a density of 5×10^5 cells per 100-mm dish. After overnight incubation, the cells were treated with (*Th*) or without (control) *T. hirsuta* extract at the indicated dilution for 48 h. The synthesized melanin was then extracted and measured as described in the Materials and methods. The quantified melanin content was divided by the viable cell number. The treated cells were also assayed for cell viability as described in the Materials and methods. The bar graph indicates melanin content (left-hand *y*-axis). The line graph indicates cell viability (right-hand *y*-axis). Results represent means ± SD of triplicate samples. *Statistically significant ($P < 0.001$) difference between *T. hirsuta* extract-treated cells and control.

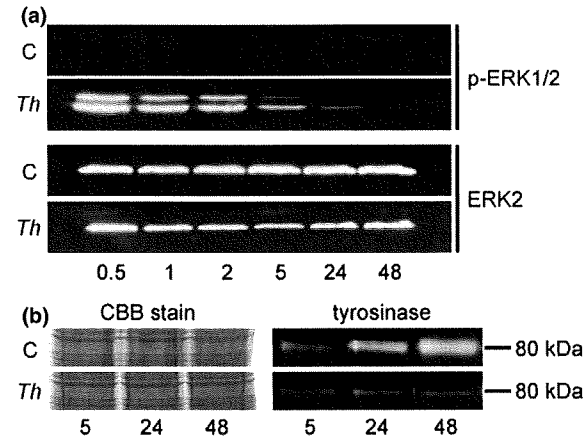

Figure 2. Effect of *T. hirsuta* extract on protein expression by B16 murine melanoma cells. (a) ERK1/2 phosphorylation in B16 murine melanoma cells treated with *T. hirsuta* extract. B16 cells were seeded at a density of 3×10^6 cells per 100-mm dish. After overnight incubation, the cells were treated with (*Th*) or without (C) *T. hirsuta* extract at 300-fold dilution for indicated time. Total proteins were then extracted and resolved by SDS-PAGE and the resolved proteins were then blotted onto a nitrocellulose membrane. The phosphorylated ERK1/2 extracted from the B16 cells was detected by immunoblotting with anti-activated ERK1/2 monoclonal antibody (upper panel) and anti-ERK1/2 monoclonal antibody (lower panel). The signal was visualized using the Immobilon Western Chemiluminescent HRP Substrate. The numbers below the panels indicate treatment time (h). (b) Tyrosinase expression levels in B16 murine melanoma cells. B16 cells were seeded at a density of 3×10^6 cells per 100-mm dish. After overnight incubation, the cells were treated with (*Th*) or without (C) *T. hirsuta* extract at 300-fold dilution for 5, 24 and 48 h. Total proteins were then extracted and resolved by SDS-PAGE; the resolved proteins were then blotted onto a nitrocellulose membrane (right panel) or stained with CBB dye as loading control (left panel). The tyrosinase extracted from B16 cells was detected by immunoblotting with anti-tyrosinase polyclonal antibody. The signal was visualized using the Immobilon Western Chemiluminescent HRP Substrate.

antimelanogenesis in B16 cells treated with the extract, we performed Western blotting to determine ERK1/2 phosphorylation (Fig. 2a).

Total protein was extracted from B16 murine melanoma cells treated with or without the *T. hirsuta* extract. To obtain sufficient protein for Western blotting, more cells are required. Thus, we used 3×10^6 cells as the initial cell number. To maintain the same treatment condition as that of the melanin quantification assay, the B16 cells were treated with the *T. hirsuta* extract at 300-fold dilution.

Although the expression levels of ERK2 in cultured B16 cells were not affected by treatment with the extract (Fig. 2a, lower panel), the phosphorylation of ERK1/2 in B16 cells was considerably enhanced after 0.5–5 h of treatment with the extract (Fig. 2a, upper panel). This result indicated that the antimelanogenesis effect of the extract in B16 cells is associated with ERK1/2 phosphorylation. The MAPK cascade is one of the most important intracellular signal transduction cascades, and many important signals are transduced to the nucleus via this cascade. Based on the phosphorylation of ERK1/2 after a short treatment time, the antimelanogenesis component might be able to interact directly with ERK1/2. The results showing the

relationship between the antimelanogenesis effect of *T. hirsuta* and ERK1/2 phosphorylation suggest that the extract may contain components that can stimulate ERK1/2 phosphorylation or regulate growth factor expression, transcription and translation.

Downregulation of tyrosinase expression by *T. hirsuta* extract

To determine the tyrosinase expression level of cells treated with *T. hirsuta* extract, we performed Western blot analysis (Fig. 2b). The tyrosinase expression levels of non-treated control cells as well as those treated for 5 h with 300-fold diluted extract were similar (Fig. 2b, right upper panel). However, cells treated for 24 and 48 h with the extract showed considerable reductions in tyrosinase expression levels (Fig. 2b, right lower panel).

These results suggest that the antimelanogenesis effect of the extract on B16 cells is associated with the downregulation of tyrosinase, the most important enzyme in melanogenesis. Moreover, the downregulation of tyrosinase by the extract requires a long treatment time of more than 5 h, and the downregulated tyrosinase expression level continues for at least 48 h.

Major compounds having antimelanogenesis activity in the *T. hirsuta* extract

To identify the major compound responsible for the activity, leaves of *T. hirsuta* was extracted in MeOH and the extract was partitioned with EtOAc, BuOH and water. We examined the effect of each layer on the melanogenesis of B16 cells and found that the EtOAc layer showed a dose-dependent antimelanogenesis activity (data not shown). The EtOAc layer was subjected to SiO_2 column chromatography to afford 17 fractions (*Th*-EtOAc-1–17) and *Th*-EtOAc-11 possessed the highest antimelanogenesis activity (data not shown). *Th*-EtOAc-11 was further fractionated into six fractions (*Th*-EtOAc-11-1–6) by a Sep-Pak ODS and *Th*-EtOAc-11-3 strongly inhibited melanin synthesis (Fig. 3). The NMR analysis revealed that the main component of the *Th*-EtOAc-11-3 fraction showed patterns which are identical to those of the typical charts of daphnane diterpenoids (15). The *Th*-EtOAc-11-3 was further separated by reversed-phase HPLC to give 15 fractions (*Th*-EtOAc-11-3-1–15) and each fraction was analysed by ^{1}H-NMR and EIMS. *Th*-EtOAc-11-3-6: EIMS *m/z* 602 (M^+), ^{1}H-NMR ($CDCl_3$, 500 MHz): δ7.60–7.75 (m, aromatic-H), 7.50 (s, 1H), 5.28 (s, 1H), 5.05 (s, 2H), 4.95 (d, J = 2.5 Hz, 1H), 4.25 (s, 1H), 3.90 (m, 1H), 3.85 (d, J = 5.4 Hz, 2H), 3.63 (br s, 1H), 2.63 (q, J = 7.3 Hz, 1H), 1.88 (s, 3H), 1.75 (d, J = 2.6 Hz, 3H), and 0.88 (m, 3H). Comparison of these data with previously published data indicated that *Th*-EtOAc-11-3-6 was identified with genkwadaphnin (16). *Th*-EtOAc-11-3-8: EIMS *m/z* 628 (M^+), ^{1}H-NMR ($CDCl_3$, 500 MHz): δ7.60–7.75 (m, aromatic-H), 7.50 (s, 1-H), 6.37 (d, J = 16.0 Hz, 1H), 5.18 (s, 1H), 5.05 (s, 2H), 4.95 (d, J = 2.5 Hz, 1H), 4.25 (s, 1H), 3.90 (m, 1H), 3.85 (d, J = 5.4 Hz, 2H), 3.63 (br s, 1H), 2.52 (q, J = 7.3 Hz, 1H), 1.88 (s, 3H), 1.75 (d, J = 2.6 Hz, 3H), and 0.88(m, 3H). Comparison of these data with previously published data revealed that *Th*-EtOAc-11-3-8 was identified with gnidicin (15).

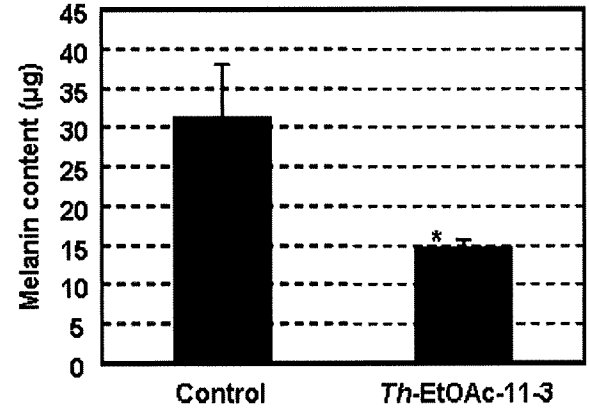

Figure 3. Synthesized melanin content in B16 murine melanoma cells. B16 cells were seeded at a density of 5×10^5 cells per 100-mm dish. After overnight incubation, the cells were treated with (*Th*-EtOAc-11-3) or without (control) fr.11-3 from the *T. hirsuta* EtOAc layer at a concentration of 0.5 µg/ml for 48 h. The synthesized melanin was then extracted and measured as described in the Materials and methods. Columns and bars represent means ± SD of triplicate samples. *Statistical significance ($P < 0.05$) between treated and control cells.

Discussion

Melanoma is the deadliest form of skin cancer and one of the most challenging of human cancers. This cancer is the fifth and sixth most common cancer among men and women, respectively. Recently, the demand for antimelanogenetic agents has increased all over the world, not only for anticancer uses but also for cosmetics as well. Choi et al. showed that an extract of *Lepidium apetalum* inhibited pigmentation via interleukin-6 signalling pathway (17). Solano et al. (2006) recently reviewed antimelanogenic agents and their specific molecular mechanisms, particurarly tyrosinase inhibition and antioxidative effects (18). Many researchers have also reported on the antimelanogenesis effects of some agents namely, 3,4-dihydroxyacetophenone (19), 4,4′-dihydroxybiphenyl (20), phospholipase D1 (21), phospholipase D2 (22), 4-*n*-butylresorcinol (23), miconazole (24), glycolic acid and lactic acid (25). This is because, depending on the age, melanin-rich spots occur on the skin and many people want to remove these spots. Thus, we would like to search for new agents that can regulate melanogenesis. There are many types of skin diseases aside from melanoma and melanin spots, such as vitiligo, porphyritic amiroidosis and hemochromatosis. Our main objective is

